From Department of Clinical Science, Intervention and Technology
Karolinska Institutet, Stockholm, Sweden

INVESTIGATION OF TUMOUR/STROMA CROSSTALK IN PANCREATIC CANCER BY AN ADVANCED 3D CO-CULTURE MODEL

Xinyuan Liu

Karolinska Institutet

Stockholm 2022

Published by Karolinska Institutet.
Printed by Universitetsservice US-AB, 2022

ISBN 978-91-8016-667-6

Investigation of tumour/stroma crosstalk in pancreatic cancer by an advanced 3D co-culture model
THESIS FOR DOCTORAL DEGREE (Ph.D.)

By

Xinyuan Liu

The thesis will be defended in public at Room Ekerö, Novum, floor 6D, Hälsovägen 7, Karolinska Institutet, Flemingsberg (Huddinge) on June 22, 2022 at 13:00.

Principal Supervisor:
Associate Professor Rainer Heuchel
Karolinska Institutet
Department of Clinical Science, Intervention and Technology
Division of Surgery

Co-supervisor(s):
Professor Matthias Löhr
Karolinska Institutet
Department of Clinical Science, Intervention and Technology
Division of Surgery

Professor Anthony Wright
Karolinska Institutet
Department of Laboratory Medicine
Division of Clinical Research Center

Opponent:
Professor Stig Linder
Karolinska Institutet & Linköping University
Department of Oncology-Pathology & Biomedical and Clinical Sciences

Examination Board:
Associate Professor Carsten Daub
Karolinska Institutet
Department of Department of Biosciences and Nutrition

Associate Professor Jonas Fuxe
Karolinska Institutet
Department of Laboratory Medicine

Professor Malin Sund
Umeå University
Department of Surgical and Perioperative Sciences

To my parents, thank you for your endless love!

ABSTRACT

Pancreatic ductal adenocarcinoma (PDAC) is one of the most lethal malignancies all over the world. This dire situation is mainly attributable to the dense desmoplasia in the tumour microenvironment (TME) and almost complete resistance to conventional chemotherapy. Cancer-associated fibroblasts (CAFs) are the key component in the TME of PDAC, which organize the excessive desmoplasia and largely affect tumour biology and treatment response. Recently, the significant heterogeneity of CAFs, regarding their origins, spatial distribution and biological function, has been discovered. However, the crosstalk between tumour cells and CAFs has been less investigated, mostly due to the lack of appropriate study models. In this thesis, we aimed to develop advanced three-dimensional (3D) co-culture models of pancreatic tumour cells and pancreatic stellate cells (PSCs, the major source of CAFs in PDAC) to dissect the interactions between tumour and stroma in PDAC.

In paper I, we first set up a heterospheroids model by directly co-culturing human PSCs (hPSCs) with human pancreatic tumour cells to study tumour/stroma crosstalk. Characterisation of the 3D co-culture model by immunohistochemistry and qRT-PCR, we discovered that the tumour cells had increased proliferation and an epithelial–mesenchymal transition phenotype upon co-culture with hPSCs. In addition, human PSCs also got activated towards a more myofibroblastic phenotype. Furthermore, a mixed-species heterospheroids model of PDAC cells and PSCs that allowed to detect the gene expression in specific cell types was developed, which confirmed the discoveries that we detected from the same-species heterospheroids model.

In paper II, we analysed the tumour/stroma crosstalk at a global transcript level by the heterospecies heterospheroids model made up of the human pancreatic tumour cells Panc1 and the mouse PSCs (mPSCs) cultured under different serum/nutrient conditions. We discovered that Panc1 shifted from the classical to the basal-like subtype upon co-culture with mPSCs independent of serum condition. In addition, mPSCs acquired different CAF phenotypes upon co-culture with Panc1 under different serum conditions. Besides, mPSCs affected the chemosensitivity of Panc1 to different drugs, increasing the sensitivity to gemcitabine but decreasing sensitivity to paclitaxel and SN38.

In paper III, we mainly investigated the function of *CCN1*, which had a significantly higher expression level in Panc1 from heterospheroids compared to monospheroids. Knockout of *CCN1* by CRISPR-Cas9 technology in Panc1 resulted in elevated gemcitabine resistance, which was probably caused by the downregulation of gemcitabine transporting and metabolizing genes (*SLC29A1* and *DCK*). In addition, we found that lysophosphatidic acid (LPA) and transforming growth factor β1 (TGFB1) signalling increased the expression of *CCN1* in Panc1 cells. Besides, stimulation with LPA and TGFB1 also shifted mPSCs to a more myCAF-like phenotype, indicated by the increased expression level of *Acta2* but decreased expression of *Cxcl1*.

In conclusion, we developed and characterized a 3D co-culture model of human pancreatic cancer cells and mouse PSCs, which reflected key features of *in vivo* PDAC. Detecting interactions

between tumour and stroma by the heterospheroids model showed novel roles of PSCs in promoting gemcitabine sensitivity of tumour cells, suggesting potential therapeutic opportunity in remodelling CAFs in PDAC.

LIST OF SCIENTIFIC PAPERS

I. Norberg KJ, **Liu X**, Fernández Moro C, Strell C, Nania S, Blümel M, Balboni A, Bozóky B, Heuchel R, Löhr M. A novel pancreatic tumour and stellate cell 3D co-culture spheroid model. BMC Cancer. 2020 May 27;20(1):475. doi: 10.1186/s12885-020-06867-5.

II. **Liu X**, Gündel B, Li X, Liu J, Wright A, Löhr M, Arvidsson G, Heuchel R. 3D heterospecies spheroids of pancreatic stroma and cancer cells demonstrate key phenotypes of pancreatic ductal adenocarcinoma. Transl Oncol. 2021 Jul;14(7):101107. doi: 10.1016/j.tranon.2021.101107.

III. **Liu X**, Gündel B, Engelsberger V, Löhr M, Heuchel R. The crosstalk analysis between mPSCs and Panc1 cells identifies CCN1 as a positive regulator of gemcitabine sensitivity in pancreatic cancer. (Unpublished manuscript)

PUBLICATION NOT INCLUDED IN THIS THESIS

Gündel B, **Liu X**, Löhr M, Heuchel R. Pancreatic Ductal Adenocarcinoma: Preclinical in vitro and ex vivo Models. Front Cell Dev Biol. 2021 Oct 22; 9:741162. doi: 10.3389/fcell.2021.741162.

CONTENTS

LIST OF ABBREVIATIONS

2D	two-dimensional
3D	three-dimensional
ADEX	aberrantly differentiated endocrine exocrine
apCAF	antigen presenting cancer associated fibroblast
ATX	autotaxin
BSA	bovine serum albumin
CAFs	cancer associated fibroblasts
ccCK18	caspase-cleaved cytokeratin 18
CCN1/ CYR61	cellular communication network factor 1/ cysteine-rich angiogenic inducer 61
CDH1	E-cadherin
CDH2	N-cadherin
CEA	carcinoembryonic antigen
COL1A1	collagen, type I, alpha 1
CTGF	connective tissue growth factor
CXCL1	C-X-C Motif Chemokine Ligand 1
DCK	deoxycytidine kinase
DEGs	differentially expressed genes
ECM	extracellular matrix
EMT	epithelial-mesenchymal transition
Enpp2	ectonucleotide pyrophosphatase/phosphodiesterase family member 2
FACS	fluorescence activated cell sorting
FBS	fetal bovine serum
FN1	fibronectin 1
FOLFIRINOX	folinic acid/leucovorin, 5-FU, irinotecan and oxaliplatin
GEMMs	genetically engineered mouse models
GSEA	gene set enrichment analysis
Hh	hedgehog
HMGCR	3-Hydroxy-3-Methylglutaryl-CoA Reductase
hPSCs	human pancreatic stellate cells
iCAF	inflammatory cancer associated fibroblast
IFNα	interferon alpha
IFNγ	interferon gamma
IGF1	insulin-like growth factor 1
IGO	intra-ductally grafted organoid
IHC	immunohistochemistry
IL-1	interleukin-1
IL1R1	interleukin 1 receptor type 1
IL-6	interleukin-6
IPMN	intraductal papillary mucinous neoplasm
ITS-A	insulin-transferrin-selenium-sodium pyruvate solution
KO	knockout
KPC	LSL-$Kras^{G12D/+}$;LSL-$p53^{R172H/+}$;Pdx1-Cre
LDLR	low-density lipoprotein receptor
LPA	lysophosphatidic acid
MCN	mucinous cystic neoplasm
MDSCs	myeloid-derived suppressor cell
mPSCs	mouse PSCs
myCAF	myofibroblastic cancer associated fibroblast
NC	negative control
OGO	orthotopically grafted organoid
PAC	paclitaxel

PanIN	pancreatic intraepithelial neoplasia
PARP	poly ADP-ribose polymerase
PC	pancreatic cancer
PCSK9	proprotein convertase subtilisin/kexin type 9
PDAC	pancreatic ductal adenocarcinoma
PDGFs	platelet-derived growth factors
PDX	patient-derived xenograft
PSCs	pancreatic stellate cells
QM-PDA	quasi-mesenchymal pancreatic ductal adenocarcinoma
qRT-PCR	quantitative real-time PCR
RNAi	RNA interference
RNA-seq	RNA sequencing
RPKM	reads per kilobase of transcript per million mapped reads
scRNA-seq	single cell RNA sequencing
SLC29A1	solute carrier family 29 member 1 (augustine blood group)
SMO	smoothened
TEM	transmission electron microscopy
TGFB1	transforming growth factor beta 1
TGFBR1/2	TGF-β receptor type I/II
TME	tumour microenvironment
VIM	vimentin
αSMA/ACTA2	alpha smooth muscle actin/ actin alpha 2, smooth muscle

1 INTRODUCTION

1.1 Epidemiology of pancreatic cancer

The global burden of pancreatic cancer (PC) has increased a lot during the past decades. The incident cases in 1990 was 195 000, and raised up to 448 000 cases in 2017[1]. This increased incidence might be because of the generally prolonged life expectancy and improved diagnosis[2]. North America and Europe have the highest incidence, followed by Argentina, East Asia and Australia (Fig.1)[2]. The survival rate of PC is very low. Although a lot of efforts had been made by doctors and scientists all over the world during the past 20 years, the 5-years survival rate increased very slowly, from 4% to 11%[1,3]. This dire situation can be ascribed largely to the late diagnosis, rapid progression, and lack of proper therapy[4-6]. Now, pancreatic cancer is one of the most lethal solid malignancies worldwide, which ranks as the fourth leading cause of cancer death in the USA and is predicted to be the second leading cause of cancer-related mortality in 2030[7,8].

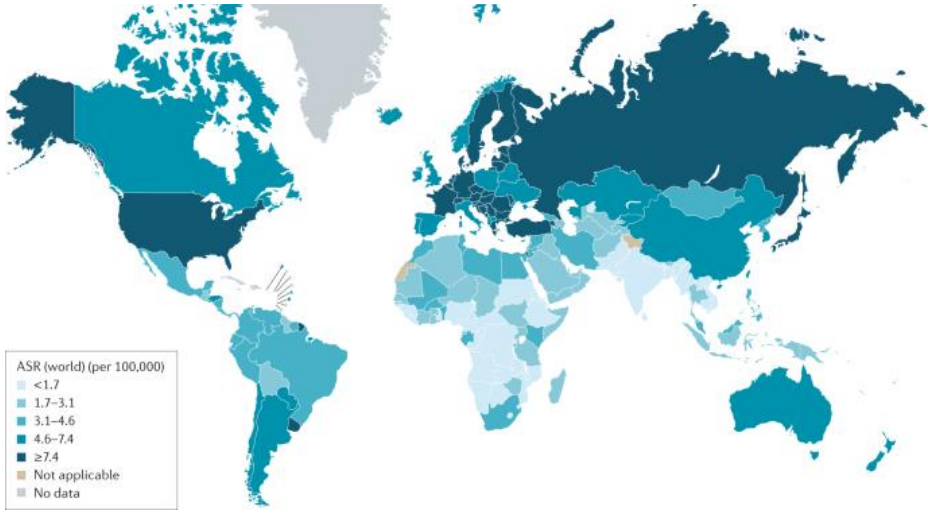

Fig.1 The worldwide incidence of pancreatic cancer in 2020 (Taken from[2]).

1.2 Risk factors of pancreatic cancer

The risk factors for pancreatic cancer include age, cigarette smoking, obesity, alcohol use, diabetes, pancreatitis and allergy[1,2]. Recently, the oral microbiota has been found related to increased risk for pancreatic cancer[9,10]. In addition, the inherited genetic factors, including pathogenic variants of *BRCA1*, *BRCA2*, *PALB2*, *ATM*, *CDKN2A*, Lynch syndrome (MLH1, MSH2 and MSH6), Peutz–Jeghers syndrome (STK11) and hereditary pancreatitis (*PRSS1)*, also play important roles in pancreatic cancer[11].

1.3 Precursor lesions of pancreatic cancer

Pancreatic ductal adenocarcinoma (PDAC) is the most common histological subtype and accounts for up to 90% of PC[12]. The precursor lesions of pancreatic cancer include the non-cystic lesion [pancreatic intraepithelial neoplasia (PanIN)] and cystic lesions [intraductal papillary mucinous neoplasm (IPMN) and mucinous cystic neoplasm (MCN)] (Fig.2)[13]. PanINs, characterized by small mucinous-papillary intraepithelial neoplasm with a ductal phenotype, are the most common precursor form of PDAC[14-16]. PanINs are classified as low grade (PanIN-1A and PanIN-1B), intermediate grade (PanIN-2) and high grade (PanIN-3), which indicate progressive neoplastic morphological changes[15,17]. KRAS oncogene mutations and telomere shortening arise early in lower grade PanIN lesions. Mutations of tumour suppressor genes, CDKN2A (P16-INK4A), SMAD4 and TP53, appear in higher grade PanINs and PDAC[18]. IPMN, characterized as large cystic neoplasm (≥5mm), is a less frequent precursor of PDAC[19]. The most common genetic alterations of IPMN are KRAS, GNAS and RNF43[13]. MCN is characterized as a composition of mucin-producing epithelial cells and an ovarian-type stroma, which arises mainly in females[19]. MCN harbours the genetic alterations found also in other precursors like KRAS, TP53, CDKN2A and SMAD4, but not GNAS[13].

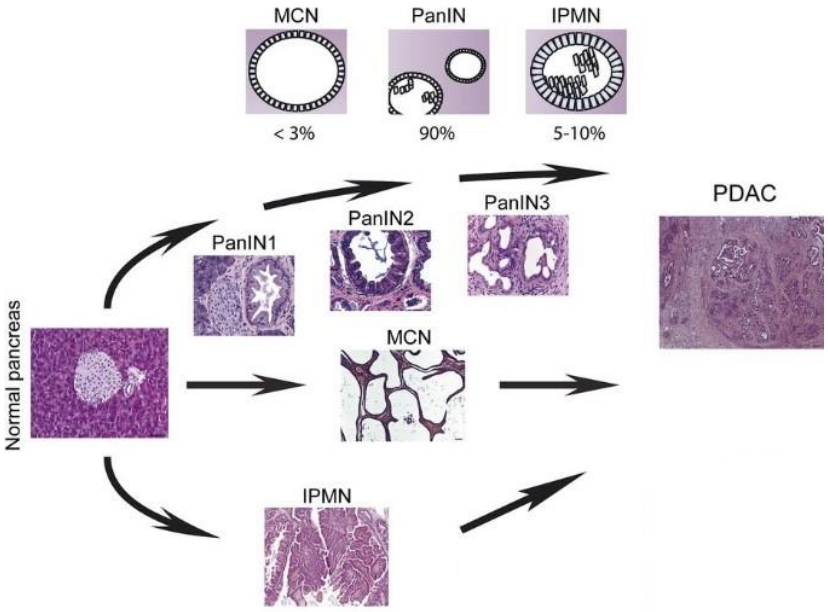

Fig.2 Diagrammatic sketch shows development of precursor lesions of PDAC (Adapted from[20]).

1.4 Current treatment of pancreatic cancer

Surgery followed by adjuvant chemotherapy is the standard treatment for patients with resectable PDAC[5]. However, only 20% of patients are eligible for resection, and most patients have a recurrence within a year[5]. Even after resection, the median survival is less than 2 years[5]. The reasons can be attributed to initially undetected micrometastasis, adverse therapeutic results by adjuvant surgical treatment and drug resistance[6]. Systemic chemotherapy is the staple therapy for patients with the unresectable disease[21]. The new first-line therapies for metastatic PDAC patients

are gemcitabine plus nanoparticle albumin-bound paclitaxel (nab-paclitaxel) and FOLFIRINOX (a combination of folinic acid/leucovorin, 5-FU, irinotecan and oxaliplatin)[22,23]. Although these therapeutic drugs are effective for advanced and metastatic PDAC patients, the development of chemoresistance severely impairs the effectiveness and contributes to the poor prognosis[6]. Recently, targeted therapy has been identified to be beneficial for a small fraction of pancreatic cancer patients. The metastatic patients who harbour germline *BRCA1/2* mutations are eligible for poly ADP-ribose polymerase (PARP) inhibitor, olaparib[24]. Patients with NTRK and NRG1 gene fusions seem to respond to tyrosine kinase inhibitors, larotrectinib and afatinib, respectively[25,26]. In addition, immunotherapy (Pembrolizumab, Anti-PD1) seems to be useful for pancreatic cancer patients with mismatch repair deficiency and microsatellite instability[27]. Recent research indicated that the tumour microenvironment (TME) has a great influence on chemoresistance in PDAC[28]. Therefore, it is urgently needed to better understand the roles of TME.

1.5 The molecular classifications of PDAC

The molecular classification of PDAC based on transcriptomic expression has been the focus of recent research. Collisson et al. firstly defined the molecular subtype of PDAC as classical, quasi-mesenchymal (QM-PDA) and exocrine-like based on gene-expression microarrays for primary epithelium microdissected tumour tissues[29]. Latterly, Moffitt et al. identified classical and basal-like subtypes of tumour, as well as normal and activated subtypes of stroma by a sophisticated computational approach on PDAC DNA microarray and RNA-seq data[30]. Bailey et al. further stratified PDAC into four subtypes, including pancreatic progenitor, squamous, immunogenic and aberrantly differentiated endocrine exocrine (ADEX) subtypes[31]. The different molecular subtypes elaborated by different research labs have certain overlap. For example, QM-PDA, basal-like and squamous subtypes of classification were well aligned and related to poor survival[32]. Lately, Puleo et al. stratified the tumour component into pure classical, immune classical, and pure basal-like. They also introduced the desmoplastic and stroma activated subtypes that were influenced by the tumour microenvironment[33]. The pure classical subtype and pure basal-like subtype were analogue to Moffitt´s classical and basal-like samples respectively[30]. Recently, Chan-Seng-Yue M et al. classified PDACs into basal-like A, basal-like B, classical-A, classical-B, and hybrid tumour clusters by bulk RNA-seq[34]. In addition, they also indicated the intratumoural heterogeneity of PDAC, since they found the classical and basal-like clusters within the same tumour by single cell RNA sequencing (scRNA-seq)[34]. Taken together, the transcriptional subtyping classified PDAC into two broad consensus classes: squamous and classical–pancreatic (Fig.3)[35].

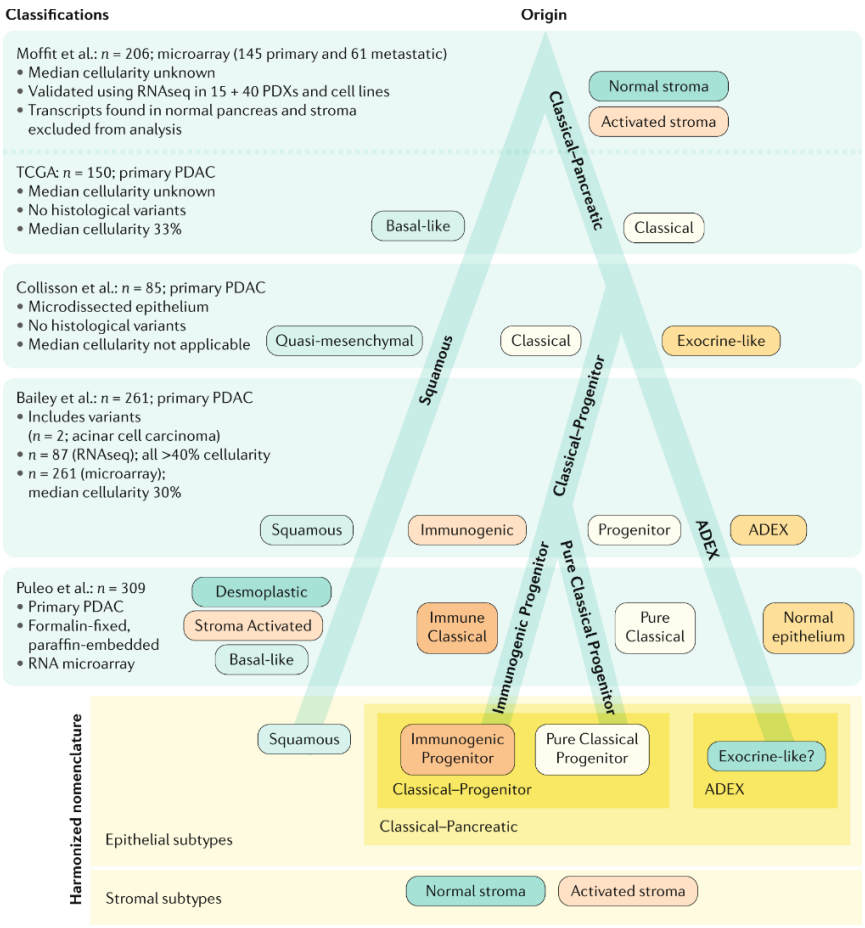

Fig. 3: Phylotranscriptomic tree of PDAC summarizes subtypes of PDAC from different studies (Taken from[35]).

1.6 The TME of PDAC

The TME is generally considered a driving force in PDAC progression, affecting metabolism, immunosuppression, metastasis and chemoresistance[36]. The TME comprises tumour cells, cancer associated fibroblasts (CAFs), immune cells, bone marrow derived mesenchymal stem cells, blood, lymph vessels and nerves, as well as extracellular matrix (ECM) components, growth factors, and cytokines (Fig.4)[36,37]. PDAC is characterized by a very dense desmoplasia, occupying in extreme cases up to 90% of the tumour volume, which results in a compressed intratumoural vasculature of PDAC[38,39]. The low functionality of intratumoural vasculature together with the high interstitial fluid pressure caused by collagen and hyaluronic acid rich ECM make diffusion difficult and lead to a nutrient, growth factors poor and hypoxic TME[39,40].

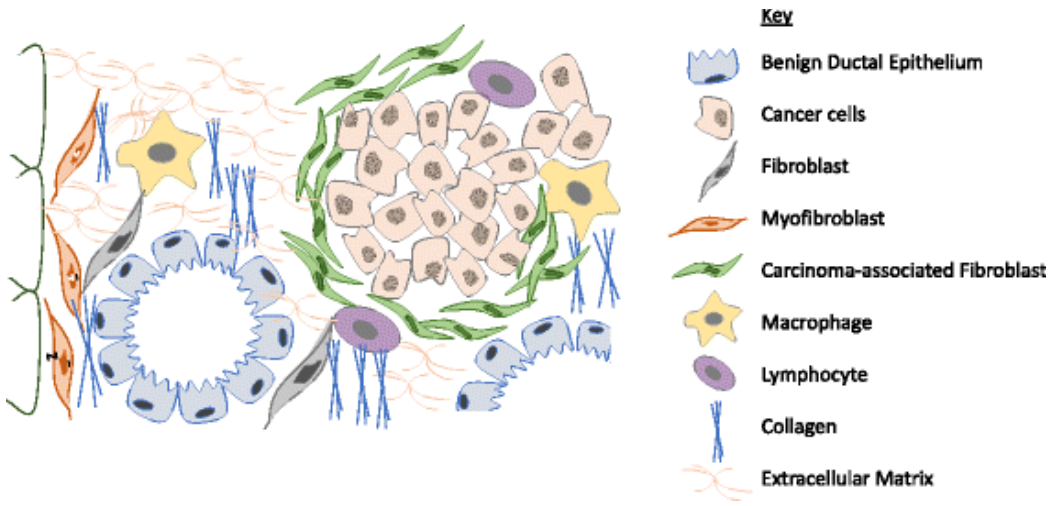

Fig. 4: The tumour microenvironment of PDAC (Taken from[41]).

1.6.1 CAFs

CAFs are the crucial component of the desmoplastic stroma, which together with other stromal components make the tumour appear like a wound that never heals[36,42]. The origin of CAFs in PDAC is difficult to define since precision specific tracking markers are lacking. The activation of resident fibroblasts is an important portion of CAFs[43]. In addition, mesenchymal stem cells, mesothelial cells, adipocytes, circulating bone marrow cells, as well as epithelial cells have also been found to have the ability to transition into CAFs[44]. The markers of CAFs include alpha smooth muscle actin(α-SMA/ACTA2), fibroblast activation protein, fibroblast-specific protein1, and platelet-derived growth factor receptor alpha and/or beta[45]. However, these biomarkers are not unique and vary for different CAFs[36].

Pancreatic stellate cells (PSCs) are the major source of CAFs[46]. In the normal pancreas, PSCs are quiescent, located in the periacinar region and contain abundant vitamin A droplets[47,48]. During PDAC development, a variety of stimulators like Interleukin-1 (IL-1), Interleukin-6 (IL-6), chemokine (C-X-C motif) ligand 2, platelet-derived growth factors (PDGFs), endothelin, hypoxia via the hypoxia inducible factor 1α, and transforming growth factor beta (TGFB) activate PSCs to a myofibroblast-like phenotype[49]. Consequently, PSCs lose the vitamin A droplets, express αSMA and acquire proliferative capacity[49]. Activated PSCs also communicate with tumour cells by secreting TGFB, IL-6, stromal cell-derived factor-1, hepatocyte growth factor and galectin-1, thus promoting PDAC progression[50].

1.6.2 CAF functions

The CAFs in PDAC have diverse functions in supporting or suppressing tumourigenesis, which depend on CAF subtypes, tumour stage and tumour genotype.

1.6.2.1 Tumor-promoting functions

The reciprocal signalling networks between CAFs and tumour cells promote PDAC progression. An in-depth phosphoproteomic analysis identified that pancreatic epithelial cells harbouring mutant $KRAS^{G12D}$ secreted SHH, which signalled to CAFs and increased CAFs secreted growth factors such as insulin-like growth factor 1 (IGF1) and growth arrest-specific gene 6[51]. In turn, CAFs stimulated phosphorylation of IGF1 receptor, AXL/TYRO3, and AKT in the pancreatic epithelial cells with mutant $KRAS^{G12D}$ and promoted PDAC proliferation[51]. In addition, CAF-derived paracrine factors, like LIF and TGFB1, act on pancreatic tumour cells and upregulate STAT3 and MAPK signalling, contributing to PDAC tumourigenesis, progression and chemoresistance[52,53]. CAFs also provide metabolic support for the proliferation of tumour cells, especially in a hypovascular and nutrient poor TME. A previous study had identified that CAFs secreted alanine, which supported lipid and non-essential amino acid biosynthesis in tumour cells[54]. CAFs also secrete specific lipid species including lysophosphatidylcholines, which could be taken up by tumour cells[55]. The exosome is another mediator that transfers amino acids and TCA cycle intermediates to tumour cells[56]. In addition to biomass production, CAFs secrete deoxycytidine that increasing the gemcitabine resistance of PDAC cells[57]. CAFs were found to take up active gemcitabine which then limited its availability to cancer cells[58]. In addition to crosstalk with tumour cells, CAFs also interact with the immune cells, which build an immunosuppressive TME in PDAC. Specifically, CAFs restrict anti-tumour T cell responses by secreting CXCL12, which excludes T cells from the tumour[59]. Beyond T cells, CAF-derived IL6 acts on monocyte precursors and promotes them to differentiate into myeloid-derived suppressor cells (MDSCs)[60]. In addition, CAFs secrete thymic stromal lymphopoietin to induce the pro-tumourigenic Th2 responses through dendritic cells conditioning[61].

1.6.2.2 Tumor-suppressive functions

Since the widely observed tumour supporting functions of CAFs, studies aiming at ablation of CAFs by different approaches, genetic or pharmacologic, had been conducted. Conditionally deleting Shh-dependent CAFs by crossing an Shh-floxed allele to *Pdx1-Cre;Kras$^{LSL\text{-}G12D/+}$;Trp53$^{fl/+}$;Rosa26$^{LSL\text{-}YFP/+}$* mouse model showed faster progression and more frequent metastasis in PDAC[62]. In addition, long term pharmacologic inhibition of canonical Hedgehog (Hh) signalling by smoothened (SMO) inhibitor IPI-926 in *LSL-Kras$^{G12D/+}$;LSL-p53$^{R172H/+}$;Pdx1-Cre* (KPC) mice also yielded poorly differentiated tumours and shortened survival[62]. Lee et al. had a similar finding that conditional deletion of Shh in pancreatic epithelial cells from the *Ptf1a-Cre;Kras$^{LSL\text{-}G12D/+}$* mouse model enhanced PanIN and PDAC formation[63]. Pharmacological inhibition or activation of Shh-Smo signalling resulted in increased or reduced epithelial cell proliferation and neoplastic progression, respectively[63]. Ablating Shh-dependent CAF by pharmacologic therapy for PDAC patients also showed disappointing results in clinical trials[64]. In addition to a Shh-devoid stroma, selective depletion of proliferating αSMA^{+} myofibroblasts by crossing *Ptf1a-Cre;Kras$^{LSL\text{-}G12D/+}$;Tgfbr2$^{flox/flox}$* model with αSMA-tk transgenic mice in combination

with systemic ganciclovir administration yielded poorly differentiated tumours and shortened survival as well[65]. Further studies suggested that αSMA-positive CAFs acted to restrain tumour progression, most probably through production of type I collagen that physically limited tumour spread[66,67]. Patients with high stromal content had been found associated with favourable outcomes in resected PDAC[68]. These studies suggested that there are sub-populations of CAFs, e.g. Shh-dependent, αSMA-positive and/or type I collagen secreting, which are able to restrain PDAC growth[69].

1.6.3 Transcriptional heterogeneity of CAFs

Öhlund et al. firstly discovered two subtypes of CAFs, myofibroblastic CAF (myCAF) and inflammatory CAF (iCAF) in PDAC through a co-culture model of PDAC organoids with PSCs[38]. The myCAF is located proximal to the cancer buds and highly expressed a-SMA/ACTA2. The iCAF is located more distal to tumour cells and with low expression level of α-SMA but high expression levels of inflammatory mediators, such as IL-6, LIF and C-X-C Motif Chemokine Ligand 1 (CXCL1)[38]. A later study elucidated a possible mechanism for the iCAF and myCAF formation, which were caused through paracrine signals of IL-1 and TGFB1 that were secreted by pancreatic tumour cells[70]. Specifically, tumour derived IL1 binding to IL1R on CAFs, which activated NF-κB signalling and subsequently prompted LIF expression and downstream JAK/STAT activation, drived iCAF generation[70]. Tumour derived TGFB activated the TGFB signalling in myCAF adjacent to tumour cells and at the same time inhibited induction of the iCAF phenotype by decreasing interleukin 1 receptor type 1 (IL1R1) expression[70]. The myCAF subtype was also found in patient tissue specimens from precursor lesions of PDAC[71]. Furthermore, Elyada et al. identified a third CAF sub-cluster, the antigen presenting CAF (apCAF) through scRNA-seq analysis of PDAC samples from patients and the KPC mouse model[72]. This CAF sub-cluster expressed class II MHC and CD74 and had putative immune-modulatory capacity[72].

1.6.4 Methods to study CAFs

The scRNA-seq is a very informative method to recognize different cell types and even subclasses of cell types within a tissue[73]. However, the lengthy isolation procedures to receive single cells change the expression profile, for example, by inducing a strong stress response[74]. In addition, certain more treatment-sensitive cells might be selectively lost during this dissociation process. CAFs are commonly under-represented in scRNA-seq analysis due to the difficulties of isolation from highly fibrotic tissues[75]. Recently, spatial transcriptomics which can be used to visualize and quantitatively analyse the transcriptome with spatial resolution in individual tissue sections has been developed[76]. Nevertheless, this method has a relatively low resolution, 50-100 μm, corresponding to 3-30 cells, and is extremely costly[76].

1.7 Cellular communication network factor 1 (CCN1)

CCN1, also named cysteine-rich angiogenic inducer 61 (CYR61), is a member of the CCN protein family[77,78]. CCN1 is an immediate-early gene, which can be transcriptionally activated by many growth factors, like TGFB1, PDGF and fibroblast growth factor 2[79]. Furthermore, agonists of G protein-coupled receptors e.g. lysophosphatidic acid (LPA) and stress stimuli induce CCN1 expression[79,80]. As a secreted protein, CCN1 connects with the cell surface and the extracellular matrix[81]. It has been reported that CCN1 plays important roles in embryonic development, senescence, tissue injury repair and angiogenesis[79,82]. In addition to the physiological processes, CCN1 also participates in pathological processes, such as fibrosis and cancer[83-85]. The various functions of CCN1 in different contexts are through interaction with different integrins and heparan sulfate proteoglycan receptors in a cell-type specific manner[79,82,86].

The increased expression level of CCN1 has been observed in pancreatic cancer tissues and metastatic lesions[87,88]. It has also been reported that CCN1 affects epithelial-mesenchymal transition (EMT), stemness, neovascularization and gemcitabine sensitivity in PDAC[89-91]. However, the regulatory molecular mechanisms, especially how CCN1 integrates into the signalling network between cancer cells and TME in PDAC, remain largely unknown.

1.8 The models to study tumour and stroma crosstalk in PDAC

1.8.1 *In vivo* model

Patient-derived xenograft (PDX), which maintains the histological and genomic alterations of the primary tumour, is used to predict clinical outcomes of drug treatment (personalised medicine) and to study tumour-stroma interactions[92-95]. However, getting enough tumour bearing animals for drug screening needs a long time and most patients die before that. Other drawbacks of PDX are that it lacks a functional immune system and the tumour stroma is replaced by the host (non-human origin), which limit the full representation of original tumour biology and response to the treatment[93]. Genetically engineered mouse models (GEMMs) are useful to study the development, pathophysiology, genetic drivers and the role of the immune system in different cancers. Compared to transplantation models for PDAC, GEMMs have extensive desmoplastic stroma and lower vascularization, which can thus be used to investigate PDAC cell/stroma interactions *in vivo*[94,96,97]. However, GEMMs are very expensive, labor-intensive and time-consuming[98].

1.8.2 *In vitro* models

In vitro models mostly refer to cell culture models, which have the advantage of changeable, and reproducible culture conditions and ease of investigating morphology changes, proliferation, apoptosis and many other biochemical and molecular parameters. In addition, different cell types can be cultured together to investigate their mutual influence.

1.8.2.1 Commonly used PDAC cell lines and PSCs

In pancreas cancer research, PSCs, as the major source of CAFs, are frequently chosen in various studies. PSCs can be isolated from normal pancreas or pancreatic cancer tissues by different ways, e.g. density gradient centrifugation and outgrowth method[47,99]. As PSCs alter their phenotype and go into senescence with increased passage numbers, researchers generated immortalized PSCs cell lines, such as RLT-PSC[100], TPSC[99], imPSC[101] and ihPSCs[102] by transformation with SV40 large T antigen and/or human telomerase reverse transcriptase. Many stable PDAC cell lines are used to study tumourigenesis and biology[103,104]. The main characters and mutational status of the 12 most commonly used PDAC cell lines are summarized in Table1[103,104].

Table1, The main characters of PDAC cell lines and genetic aberrations[103,104]

Cell line	Source of tumour cells	Grade	Vimentin	CEA	K-ras	p53	p16	DPC4/smad4
Capan-1	Liver metastasis	1	++	+	Mut	Mut	Mut	Mut
Capan-2	Primary tumour	1	-	-	Mut	W.t.	Mut	HD
Colo357	Lymph node	2	+	+	Mut	W.t.	W.t.	Mut
HPAF-2	Ascites	2	+	++	Mut	Mut	Mut	W.t.
Aspc-1	Ascites	2	+++	++	Mut	Mut	Mut	W.t./Mut
A818-4	Ascites	2	+++	-	Mut	Mut	Mut	W.t
BxPc3	Primary tumour	2	+	++	W.t.	Mut	Mut	Mut
Panc89	Lymph node	2	-	++	W.t./Mut	Mut	Mut	W.t.
PancTu-I	Primary tumour	3	+++	+	Mut	Mut	Mut	W.t.
Panc1	Primary tumour	3	+++	-	Mut	Mut	Mut	W.t.
Pt45P1	Primary tumour	3	+++	-	Mut	Mut	Mut	W.t.
MiaPaCa-2	Primary tumour	3	+++	-	Mut	Mut	Mut	W.t.

CEA, carcinoembryonic antigen; -, negative; +, <10%; ++,10-50%; +++,>50% of the cell stained by immunochemistry; Mut, mutated; W.t., wild type; HD, homozygous deletion.

1.8.2.2 The monolayer co-culture system

In two-dimensional (2D) monolayer culture, investigators study the crosstalk between stromal and cancer cells usually through direct or indirect co-culture methods. The direct co-culture is to culture two kinds of cells on the same plastic culture surface, which allows for physical interaction, making it possible to study the mediator(s) of molecular interaction(s), including especially juxtacrine signalling. The indirect co-culture method, including transwell plates and conditioned medium from the tumour or stroma cells, can be used to study the secretome-induced crosstalk between tumour and stroma[94,105]. Although 2D co-culture systems are the most widely used model with low-cost and time saving advantages, they do not recapitulate the microenvironment of three-dimensional (3D) cell interactions *in vivo*.

1.8.2.3 The 3D co-culture models

Recently, 3D culture models with a more complex tissue organization, which better mimick the biology *in vivo* compared to 2D monolayer culture, have increasingly been developed[94,106]. 3D cultures are valuable approaches to narrow the gap between traditional 2D cell cultures and animal

models, as well as decipher the contribution of individual components of the TME to tumour progression and chemotherapy responses[107,108]. The most commonly used 3D culture systems to study the communication between tumour and stromal cells are organoids and spheroids.

Organoids

Organoids are derived from dissociated primary tissues that are grown in growth factor-reduced matrigel and in a complex medium supplemented with multiple nutrients, growth factors and antibiotics, which maintain the tumour architecture, genetic profiles and epigenetic changes of the original tumour[106,109,110]. It was observed that orthotopic transplantation of PDAC organoids induced a collagen-rich murine stroma[110]. Co-culture of PDAC organoids with PSCs in Matrigel also led to PSCs activation, which acquired a CAF phenotype[38]. A novel multi-cell type co-culture model, based on co-culture of tumour organoids with patient-matched CAFs and lymphocytes in Matrigel, displayed increased gemcitabine resistance of tumour cells and the myCAF phenotype as well as tumour-dependent lymphocyte infiltration, suggesting the ability to reflect the complex interplay of pancreatic tumour components[111]. However, the generation and culture of organoids are costly, time consuming and less amenable for high throughput screening. The use of Matrigel also limits the reproducibility of experiment outcomes due to high batch variations.

Spheroid culture systems

Cell lines cultured in 3D to allow cells to organize into spherical structures are named spheroids[112]. Tumour spheroids display chemical gradients, including oxygen, nutrients, and catabolites, at diameters between 200 to 500 µm[113]. Cells located in the periphery of a spheroid reflect the *in vivo* situation of actively cycling tumour cells adjacent to blood supplying capillaries. In contrast, when the spheroid size is more than 500 µm, innermost cells get quiescent and eventually turn to apoptosis or necrosis[114]. The concentric arrangement of heterogeneous cell populations and the pathophysiological gradients in spheroids are similar to the situation in micrometastases, avascular tumour microregions or inter-capillary tumour nests[114]. Different ways are used to inhibit cellular attachment to plastic culture plate surfaces and thus force cells to aggregate, such as keeping cells in motion[112,115], not allowing cells to attach[116-119], or provision of some form of extracellular matrix[120-122]. These aggregation cell clusters have poor oxygen diffusion into the centre, which resembles hypoxic tumour areas[119].

The spheroids of tumour cells co-cultured with other cell types better recapitulate the tumour microenvironment[123]. It has been found that tumour-stroma spheroids showed increased ECM deposition resulting in lower diffusion of gemcitabine compared to only tumour spheroids[118]. In addition, a microarray based transcriptional analysis on the co-cultured spheroid of pancreatic cancer cells (PT45) with normal fibroblasts and CAFs showed activation of the fibroblasts upon co-culture[124]. The PSCs have been identified to induce EMT of tumour cells by using a microchannel plate-based co-culture model of Panc1 and PSC[125]. Furthermore, advanced imaging techniques like multiphoton excitation and second harmonic generation can be used on microfluidic co-culture

spheroid models of PSCs and Panc1 cells to study tumour-stroma interaction and evaluate drug efficacy[126].

1.9 Knowledge gaps

The TME provides an adaptive niche for PDAC cells, and the interaction between neoplastic cells and stromal cells has distinct effects on PDAC progression. Therefore, an in-depth understanding of the crosstalk between tumour and stroma could provide suitable strategies for stroma targeted therapy in the future. A model with high reproducibility and cost effectiveness, which better reflects the TME of PDAC, is urgently needed to study tumour/stroma interactions and test therapeutic regimens. A major challenge for studying CAFs is the difficulty of CAF isolation, which is due to the lack of specific markers and they are tightly embedded in the ECM of the tumour. Furthermore, it is difficult to analyse the expression of two or more cell types of the same species, unless single cell information is connected with spatial information. Therefore, in this study, we detected the tumour/stroma crosstalk on co-cultured spheroids model of pancreatic tumour cells and PSCs from different species by advanced bioinformatic tools without prior physical cell isolation.

2 RESEARCH AIMS

The overall goal of the thesis work is to better understand the crosstalk between pancreatic cancer cells and PSCs by using advanced *in vitro* methods that mimick pancreatic cancer and ultimately find ways to overcome the intrinsic chemoresistance.

Specific Aim 1: To build a novel pancreatic tumour and stellate cells 3D co-culture spheroid model that can investigate the tumour/stroma crosstalk in promoting pancreatic cancer carcinogenesis.

Specific Aim 2: To investigate the role of pancreatic tumour/stroma crosstalk in a global level by a "virtual sorting" analysis approach on the heterospecies heterospheroid model under different environmental conditions.

Specific Aim 3: To investigate the role of promising signalling candidates between tumour and stromal cells, and identify a potential chemoresistance mechanism in pancreatic cancer using the heterospecies heterospheroid model.

3 MATERIALS AND METHODS

The materials and methods employed in the thesis are briefly described here. For more detailed information, please see the attached Papers I-III.

3.1 Cell lines (Paper I, II and III)

The well-characterized human pancreatic cancer cell lines: Panc1 and HPAFII cells were purchased from ATCC[104]. Authentication of Panc1 cells by detecting short tandem repeat profiles was performed by ATCC with the Promega's PowerPlex® 18D System. The human pancreatic stellate cells (hPSCs) were isolated and characterized by Matthias Löhr´s previous laboratory at the DKFZ in Heidelberg, Germany[100]. The KPCT 86-2 cell line was isolated from a KPC mouse[97] that was mated to the tdTomato allele (B6.Cg-*Gt(ROSA)26Sor*$^{tm9(CAG\text{-}tdTomato)Hze}$/J)[127]. The immortalized mouse pancreatic stellate cell line clone2 and clone 3 (imPSCc2 and imPSCc3) were a generous gift by Dr. Raul Urrutia and Dr. Angela Mathison at the Mayo Clinic College of Medicine, Rochester, Minn, USA[101]. CCN1 knockout (KO) pancreatic cancer cell lines (Panc1-CCN1-KO) were generated at the Karolinska Genome Engineering core facility using the CRISPR/Cas9 technique. The knockout clones were verified by sanger sequencing and western blotting.

3.2 Monolayer cell culture (Paper I, II and III)

The cell lines including Panc1, Panc1-CCN1-KO, hPSCs, KPCT 86-2 and imPSCs (c2 and c3) were cultivated with DMEM/F12 (Gibco 31330095) medium and HPAFII was fed with RPMI-1640 medium. All cell lines were supplemented with 10% fetal bovine serum (FBS, Gibco 10270106) and 0.5% penicillin/streptomycin (Gibco 15070063) under standard culture conditions (5% CO_2, at 37°C). In paper II, Panc1 and imPSCc2 were also cultivated under low serum condition (mimicking nutrient-poor condition) supplemented with 0.1% FBS, 0.3% bovine serum albumin (BSA, only for Panc1 cells) (Sigma A9647), 0.1% (10% of the recommended concentration) insulin-transferrin-selenium-sodium pyruvate solution (ITS-A, Gibco 51300044) and 0.5% penicillin/streptomycin in a humidified incubator at 37°C and 5% CO_2. In paper II, Panc1 and imPSCc2 were stepwise adapted to the low serum condition over a course of 6–8 weeks. All cells were tested negative for mycoplasma (MycoAlertTM PLUS Mycoplasma Detection Kit, LT07-705, Lonza, Switzerland).

3.3 Spheroids systems (Paper I, II and III)

In paper I, PDAC tumour cells and PSCs from human and mouse were seeded alone (monospheroids) or in co-culture at the ratio of 1:1 (heterospheroids) with total 2500 cells/well in non-treated, round-bottom 96-well microplates (Falcon, 351177, BD NJ, USA) in DMEM/F12 medium supplemented with 10% FBS and 0.5% penicillin/streptomycin as well as 0.24%

methylcellulose at 37°C and 5% CO_2 humidified condition[119,128]. After the indicated number of days, the formed spheroid cultures were collected and processed for downstream purposes. **In paper II**, the Panc1 and imPSCc2 (hereafter called mPSCs) were grown either as monospheroids (2500 cells for each cell type) or heterospheroids (2000 cells of mPSCs and 500 cells of Panc1) in non-treated, round-bottom 96-well microplates in DMEM/F12 medium supplemented with either 10% FBS ("high serum" condition) or 0.1% FBS, 0.3% BSA and 0.1% ITS-A ("low serum" condition), and 0.5% penicillin/streptomycin as well as 0.24% methylcellulose at 37℃ and 5% CO_2 humidified condition. **In paper III**, Panc1, Panc1-CCN1-KO (C3, C7 and F3 clones), as well as mPSCs were grown either as monospheroids (2500 mPSCs or Panc1 or Panc1-CCN1-KO cells) or heterospheroids (2000 mPSCs co-cultured with 500 cells of Panc1 or Panc1-CCN1-KO) in non-treated, round-bottom 96-well microplates in DMEM medium supplemented with either high serum condition (10% FBS) or low serum condition (0.1%FBS, 0.5% fatty acid free BSA (Sigma, A8806) and 0.1% ITS-A) and 1% GlutaMAX™ supplement, 0.5% penicillin/streptomycin as well as 0.24% methylcellulose at 37℃, 5% CO_2 and under humidified condition.

3.4 Imaging by transmission electron microscopy (TEM) (Paper I)

The monospheroids and heterospheroids were collected and fixed in 2.5% glutaraldehyde and 1% formaldehyde in 0.1M phosphate buffer. Then the spheroids were rinsed in 0.1M phosphate buffer before post-fixation with 2% osmium tetroxide in 0.1M phosphate buffer, pH 7.4 at 4°C for 2 hours. The spheroids were then stepwise dehydrated in ethanol, followed by acetone and finally embedded in LX-112. Ultrathin sections (~50–60 nm) were prepared using an EM UC7 (Leica) and were contrasted with uranyl acetate followed by lead citrate. Imaging was performed by a Tecnai 12 Spirit Bio TWIN transmission electron microscope (Fei Company, Eindhoven, The Netherlands) at the electron microscopy unit of Karolinska Institutet.

3.5 Immunohistochemistry (IHC) (Paper I)

Spheroids were collected following the desired growth period, washed in phosphate buffered saline and fixed in 4% paraformaldehyde for 24 hours at room temperature. Then spheroids were transferred to biopsy cryomolds (Tissue-Tek Cryomold #4565). The HistoGel was heated up in a water filled beaker in the microwave until the gel was liquefied. About 100 µl HistoGel (ThermoFisher Scientific, HG-4000-012) was used to embed spheroids at one corner of the cryomold, and the cryomold was kept tilted on ice until the HistoGel had solidified. Then the biopsy cryomold was filled up with another 300 µl HistoGel and kept on ice to solidify the gel. After that, the solid gel was gently transferred into a biopsy cassette and kept in 70% ethanol until further processing[119,129]. Paraffin-embedded spheroids were sectioned at 4µm before hematoxylin-eosin staining or immunohistochemistry for CK19 (NCL-CK19, Novocastra Leica Biosystems Ltd), E-cadherin (05905290001, Ventana Roche), MKI67 (M7240, Dako - Agilent: Dako) and vimentin (VIM, M0725, Dako - Agilent: Dako) at the Morphological Phenotype Analysis core facility at

Karolinska Institutet. Histological slides were digitalized by a 3D Histech Panoramic SCAN II slide scanner. Quantitation of immunohistochemical markers was performed on the whole slide images using QuPath v1.3[130].

3.6 Virtual sorting (Paper I-III)

3.6.1 Species-specific reverse transcription-real time polymerase chain reaction (qRT-PCR) (**Paper I-III**)

The spheroids were collected after the desired growth period and total RNA was isolated using the QIAshredder (Qiagen) and the RNeasy Mini Kit (Qiagen) according to the manufacturer´s instructions. The concentration of RNA was measured using the NanoPhotometer® NP80. The total RNA (1 µg in Paper I or 0.25 µg in Paper II and III) was further reverse transcribed to synthesize cDNA by the iScript cDNA Synthesis kit (Bio-Rad, 1708891). In order to detect the gene expression in a specific cell type (human or mouse) in the heterospecies heterospheroids, we designed species-specific primers based on areas that are genetically diverse in the human and mouse homologues genes by NCBI Blast (https://blast.ncbi.nlm.nih.gov/) and PRIMER3 (v.0.4.0). Species-specificity of the primers was verified by testing each primer pair on cDNA preparations from both human and mouse cell lines. The PCR reaction products were further tested on a 2% agarose gel. The qRT-PCR reaction was performed using Thermo Scientific™ Maxima SYBR Green/Fluorescein qPCR Master Mix kit (ThermoFisher Scientific, K0243) following the amplification program: initial denaturation 10 minutes at 95°C, 40 cycles of 15 seconds at 95°C and 1 minute at 60°C[129]. *RPL13A*/*Rpl13a* for human and mouse served as housekeeping genes, respectively. For each gene, three independent biological replicates were performed. Gene expression was calculated by $2^{-\Delta\Delta ct}$ method. Statistical analyses based on delta CT values were conducted by Student's t-test (2-sided, individual samples).

3.6.2 RNA sequencing (Paper II)

The spheroids were collected after 5 days of growing and total RNA was extracted directly from monospheroids and heterospheroids using the QIAshredder and RNeasy PLUS kit (Qiagen). Quality assessment and quantification of RNA were performed using TapeStation (Agilent). Library preparations were conducted by the NEBNext® Ultra™ II Directional RNA Library Prep Kit (NEB, E7760S). The multiplexed libraries were sequenced using an Illumina HiSeq3000 instrument at the Integrated Cardio Metabolic Centre at Karolinska Institutet, that generating on average 20 million single-end 50 bp reads for each sample.

3.6.3 Separation of mixed reads to each species and mapping to reference genomes (Paper II)

Reference genomes for human and mouse, GRCh38.87 and GRCm38.87, downloaded from Ensembl were used to build respective indexes for the species-based read classifier Xenome (1.0.1)[131] and the short read aligner STAR (2.5.1b)[132]. The Xenome program was used to classify fastq reads to each species (Fig.5)[131]. Separated human and mouse reads were then aligned to their respective reference genomes by STAR program with default options (Fig.5)[132]. Program of featureCounts (1.5.2) was employed to quantify reads mapping to known features in the Ensembl database (Fig.5)[133].

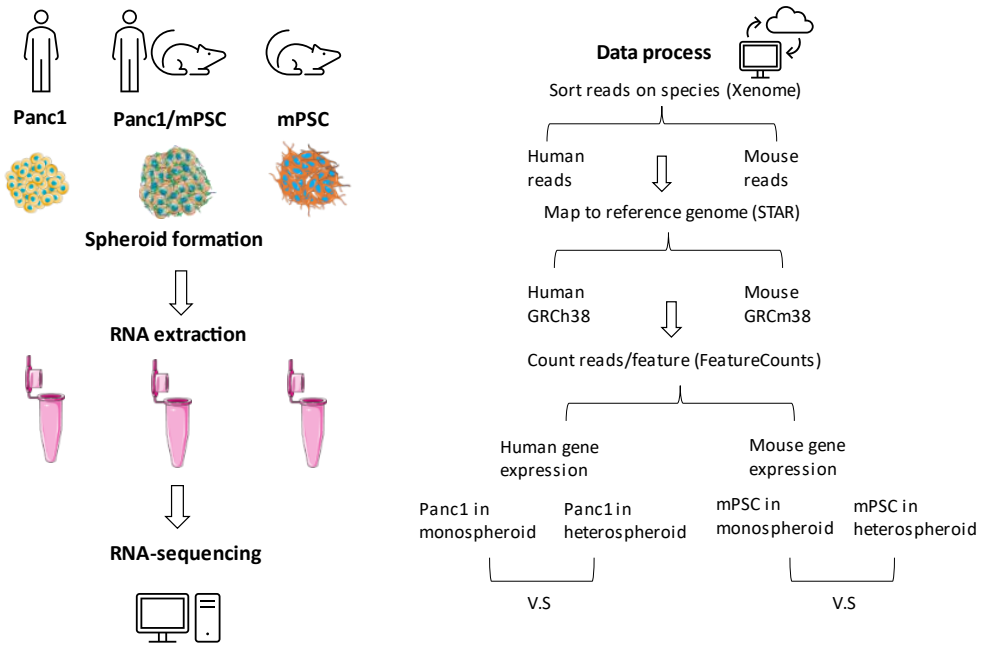

Fig.5 The schematic diagram of the virtual sorting approach for the detection of the tumour and stroma crosstalk on transcriptional level based on the mixed species heterospheroids model. (The figure was partly generated using Servier Medical Art, provided by Servier, licensed under a Creative Commons Attribution 3.0 unported license.)

3.6.4 Differential expression analysis, gene set enrichment analysis (GSEA) and molecular subtype analysis (Paper II)

The R package of edgeR (v3.30.3) was used to calculate differentially expressed genes (DEGs) between heterospheroids and monospheroids with the threshold of an FDR q-value < 0.05 and an absolute fold change > 1.5[134]. The RPKM (Reads Per Kilobase of transcript per Million mapped reads) expression levels were used for GSEA based on gene sets of hallmark (h.all.v7.1.entrez.gmt)[135] and KEGG subsets from canonical pathways (c2.cp.kegg.v7.2.symbols.gmt)[136]. The DEGs of Panc1 were compared to the classical/basal-like signatures[30], progenitor/squamous signatures[31] and chemosensitivity signatures[137] using Fisher's exact test. The DEGs of mPSCs were compared to CAF signatures[38] using Fisher's exact tests. The pheatmap (v1.0.12) R package was used to visualize the result[138].

3.7 Western Blotting (Paper III)

The protein from Panc1 cells and Panc1-CCN1-KO clones were extracted by T-PER Tissue Protein Extraction Reagent (Thermo Fisher, 78510) which contained a protease inhibitor cocktail (Roche, 05892970001). Bradford protein assay (Bio-Rad, 5000201) was further conducted to detect the protein concentration. The same amount (30 μg) of denatured protein from Panc1 cells and Panc1-CCN1-KO clones were subjected to gradient polyacrylamide gels for electrophoresis. Then Trans-Blot Turbo transfer system was employed to blot separated proteins to a nitrocellulose membrane (Bio-Rad, 1704158). Membranes were blocked in 1X Tris-Buffered Saline, 0.1% Tween-20 buffer (ThermoFisher, #28360) containing 5% BSA, and were further incubated with primary antibody: CCN1 (Boster Bio, PB9549, 1:1000), deoxycytidine kinase (DCK) (LifeSpan BioSciences, LS-B10837, 1:1000), and tubulin (Abcam, ab7291,1:1000) overnight or for 3 days at 4°C. Then fluorophore-coupled secondary antibody: goat-anti-rabbit-AlexaFluor488 (1:10000) and goat-anti-mouse-AlexaFluor647 (1:10000) were used for detection.

3.8 TGFB1 and LPA stimulation assay

In Paper III, Panc1 cells and mPSCs were grown as monospheroids in either high serum condition or low serum condition. Panc1 and mPSC monospheroids were stimulated with either 5 ng/ml recombinant human TGFB1 protein (PreproTech Nordic, 100-21-10), or 20 μM 18:1 LPA (Avanti® Polar Lipids, Inc.857130P) on day1 and harvested on day4 for RNA isolation and gene expression detection.

3.9 Inhibition of TGFB and LPA signalling

In paper II, Panc1/mPSCs heterospheroids were seeded in high serum condition and treated with 5 μM TGFB receptor type I/II (TGFBR1/2) kinase inhibitor (LY2109761, Sigma-Aldrich, #SML2051) on day 1 for 72 hours. Then spheroids were collected for RNA extraction and gene expression detection. **In Paper III**, Panc1/mPSC heterospheroids were set up in high serum condition and treated on day5 with 5 μM TGFBR1/2 kinase inhibitor LY2109761 or 10 μM autotaxin (ATX) inhibitor PF8380 (SML0715) or the combination of both inhibitors. Heterospheroids were harvested on day8 for RNA extraction and gene expression detection.

3.10 Cell viability assay (Paper III)

Panc1 cells and Panc1-CCN1-KO (C3 and C7) clones were cultured in traditional monolayer and as monospheroids under high serum condition. Different doses (1, 5 and 50 μM) of gemcitabine (Sigma-Aldrich, G6423) were treated, respectively, on day1 and cell viability was detected by the ATP-based CellTiter-Glo® 3D Cell viability assay (Promega) on day4 according to the manufacturer's protocol. The luminescence was measured by a SpectraMax i3x microplate reader.

The relative cell viability was determined by normalizing the luminescence of drug-treated cells to the respective negative control. Statistically significant differences between Panc1 cells and Panc1-CCN1-KO clones were assessed using Student's t-test (individual samples).

3.11 Epithelial-specific apoptosis assay (Paper II and Paper III)

In paper II, Panc1 monospheroids and heterospheroids were seeded in high serum condition and treated with different therapeutic compounds, including 50 µM gemcitabine, 1 µM paclitaxel (Sigma-Aldrich, 580555) and 1 µM SN38 (an active metabolite of irinotecan; Sigma-Aldrich, H0165) or 5 µM pitavastatin (an HMG-CoA reductase inhibitor; Selleckchem, #S1759) on day1 for three days. Then the epithelial-specific caspase-cleaved cytokeratin 18 (ccCK18) of each spheroid was quantitatively detected by M30 Apoptosense® CK18 Kit (Diapharma #P10011) according to the manufacturer's instructions. The relative cell apoptosis rate was determined by normalizing the ccCK18 value for drug treated spheroid to the negative control (NC), and differences between monospheroids and heterospheroids were assessed by paired t-test. **In paper III**, the epithelial-specific ccCK18 of Panc1 and Panc1-CCN1-KO monospheroids and heterospheroids, that were grown under high serum condition with 50 µM gemcitabine treatment on day1 for 72 h, was detected. The relative cell apoptosis rate was determined by normalizing the ccCK18 value for gemcitabine treated spheroid to the negative control, and differences between samples were assessed by Student's t-test.

3.12 Microarray dataset analysis (Paper III)

The mRNA microarray expression data from PDAC patients (GSE71729[30]) were downloaded from Gene Expression Omnibus by the Geoquery package[139]. The association between selected interesting genes was analysed by the linear regression method by R. The visualization was performed by the ggplot2 package[140].

4 RESULTS

4.1 Paper I

4.1.1 Heterospheroids model based on human tumour cells and human PSCs

We first set up the 3D co-culture model based on human pancreatic cancer cells Panc1 and human PSC. The morphological analysis from TEM and haematoxylin/eosin staining for both monospheroids and heterospheroids illustrated a healthy spheroid structure (Fig.6 A and B). Besides, no visible division/separation between the tumour cells and PSCs in the heterospheroid was observed. Therefore, we analysed the distribution of Panc1 and hPSCs by IHC staining of CK19, an epithelial cell specific marker, and evaluated the proliferate capacity by staining of MKI67. The results showed that Panc1 had a uniform presence of CK19, whereas hPSCs completely lacked CK19 protein expression (Fig.6C). In addition, the quantification of CK19 positive and negative cells in the heterospheroids indicated the ratio of Panc1 and hPSC fluctuated over time but stabilized at around 1:1 at later time points of Day5 and Day7 (Fig.6D). The qRT-PCR results also confirmed that the mRNA expression of CK19 was only detected in Panc1 cells while absent in hPSCs, and the reduced gene expression in the heterospheroids reflected the expected ratio of both cell types (Fig.6E). Furthermore, we found that Panc1 cells in the heterospheroids had a higher percentage of MKI67 positive cells compared to monospheroids at all time points (Fig.6F). Almost all the hPSCs were positively stained for MKI67, which was little affected by co-culture with Panc1(Fig.6F). In addition, we discovered that E-cadherin (CDH1) was partially expressed by Panc1 from monospheroids but not by hPSC (Fig.6G). Notably, the CDH1 protein was almost completely lost in the Panc1/hPSC heterospheroids (Fig.6G). Moreover, we found that both Panc1 cells and hPSCs were positively stained with the mesenchymal marker VIM (Fig.6H).

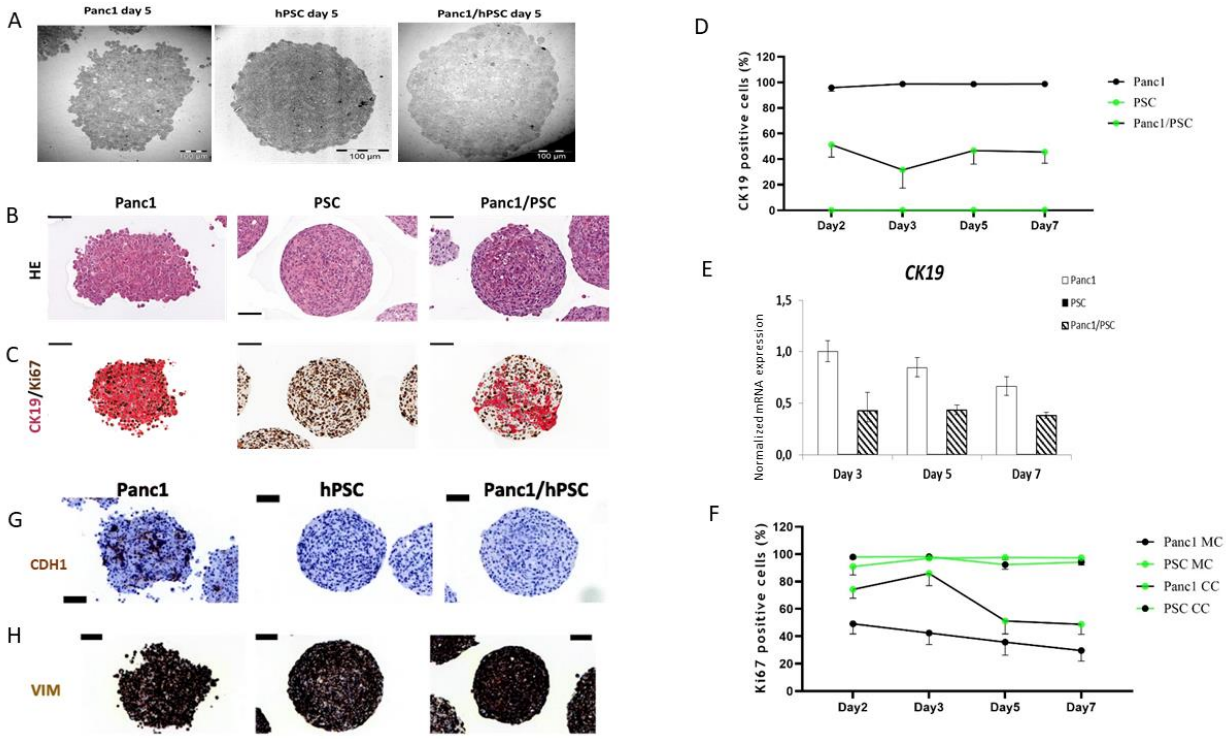

Fig.6 (A-B) Transmission electron microscopy (A) and haematoxylin and eosin-staining (B) of spheroids cultured for 5 days. (C) Representative pictures of immunohistochemical double-staining of CK19 (red) and the MKI67 of spheroids cultured for 5 days. (D) Quantification of CK19 positive staining cells from each type of spheroids. (E) Normalized mRNA expressions of CK19 in Panc1 and hPSC mono- and heterospheroids. (F) Quantification of MKI67 positive staining cells from each type of spheroids. (G-H) Representative pictures of immunohistochemical staining of CDH1 or VIM of spheroids cultured for 5 days. Black scale bars correspond to 100 µm. (Adapted from Paper I)

We also detected the mRNA expression levels of activated PSC markers *ACTA2* and fibronectin 1 (*FN1)* and found that both genes were expressed in hPSCs but not in Panc1 from monospheroids (Fig.7). In addition, the expression levels of *ACTA2* and *FN1* were comparatively upregulated upon co-culture since the total expression only came from around 40-50% of the cells in the heterospheroids (Fig.7). The expression of collagen, type I, alpha 1 (*COL1A1*) was increased in Panc1 from monospheroids over time, while it remained stable in hPSC monospheroids and Panc1/hPSC heterospheroids (Fig.7). Both Panc1 and hPSC from monospheroids expressed *TGFB1* (Fig.7), but the contribution to the *TGFB1* expression by each cell type in the heterospheroids could not be determined by this method.

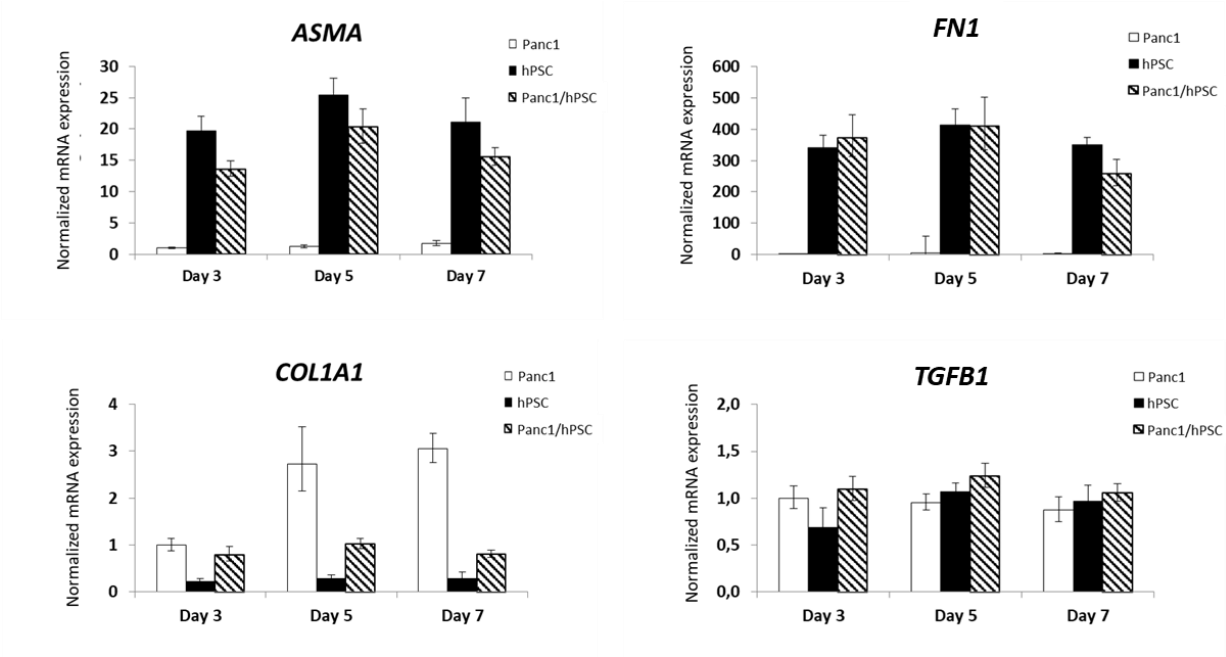

Fig.7 Normalized mRNA expressions of *ASMA* (*ACTA2*), *FN1*, *COL1A1* and *TGFB1* in Panc1 and hPSCs mono- and heterospheroids. (Adapted from Paper I)

In addition to Panc1, we also generated the spheroid model using HPAFII, another human pancreatic cancer cell line. The haematoxylin/eosin staining showed that HPAFII monospheroids formed hollow, glandular-like structures (Fig.8A), which was quite different as the Panc1 monospheroids. For the HPAFII/hPSC heterospheroids, there was a distinct separation between the two cell types (Fig.8A). By CK19 staining, we identified that the cells located in the outer ring of the heterospheroids were HPAFII cells ($CK19^{+}$) and in the core were hPSCs ($CK19^{-}$) (Fig.8B). The quantification of CK19 positive cells showed a higher ratio of HPAFII cells than hPSCs in the heterospheroids, especially on day5 (Fig.8C). In addition, we quantified the MKI67 positive cells and found a higher proportion of proliferating HPAFII in heterospheroids compared to monospheroids, while almost all hPSCs in both monospheroids and heterospheroids were proliferating (Fig.8D). Besides, we observed that vimentin was only expressed by hPSCs but not by HPAFII cells (Fig.8E). In addition, we detected the expression of the epithelial marker CDH1 and found that almost all HPAFII cells in the monospheroids expressed CDH1, but not hPSCs (Fig.8F). Notably, HPAFII cells also expressed high levels of CDH1 when co-cultured with hPSCs, which was different from the Panc1 spheroid model.

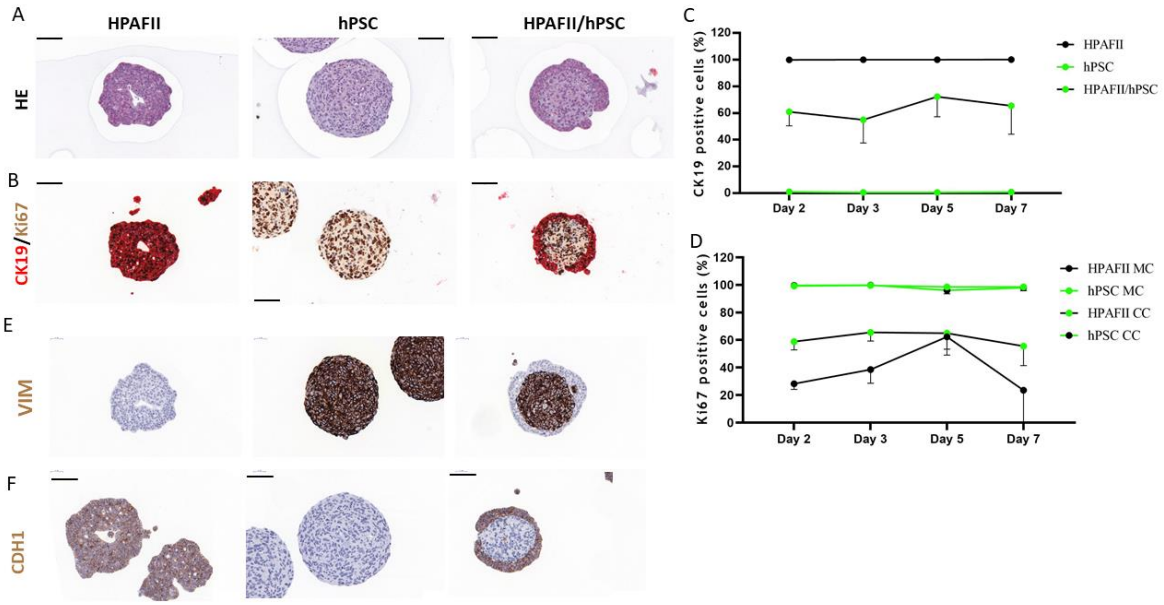

Fig.8 (A) Haematoxylin and eosin-staining of spheroids cultured for 5 days. (B) Representative pictures of immunohistochemical double staining of CK19 (red) and the MKI67 of spheroids cultured for 5 days. (C) Quantification of CK19 positive staining cells from each type of spheroids. (D) Quantification of MKI67 positive staining cells from each type of spheroids. (E-F) Representative pictures of immunohistochemical staining of VIM or CDH1 of spheroids cultured for 5 days. Black scale bars correspond to 100 µm. (Adapted from Paper I)

The qRT-PCR results showed that *ACTA2*, *FN1* and *COL1A1* were all expressed in hPSCs but not in HPAFII from monospheroids (Fig.9). In the heterospheroids, the expression levels of these three genes seemed to be increased, based on the assumption that only 40% of cells in the co-cultures were hPSCs and that HPAFII cells in the heterospheroids did not express these genes (Fig.9). In addition, both HPAFII and hPSC from monospheroids expressed *TGFB1* at the mRNA level (Fig.9). The expression of *TGFB1* was increased in heterospheroids compared to monospheroids on day 7, however, we could not identify the individual contribution of the two cell types in the heterospheroids (Fig.9).

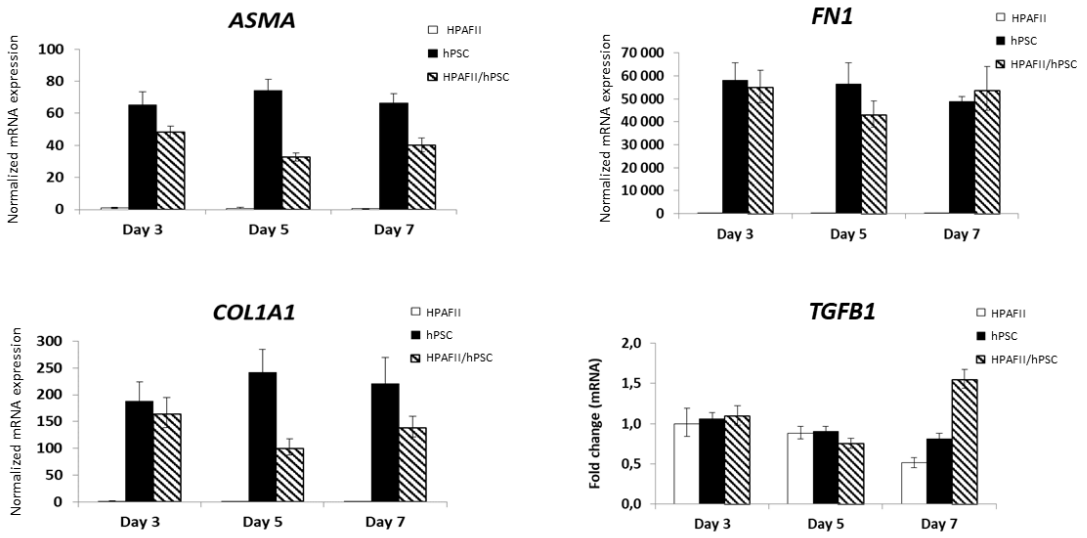

Fig.9 Normalized mRNA expressions of *ASMA* (*ACTA2*), *FN1*, *COL1A1* and *TGFB1* in HPAFII and hPSCs mono- and heterospheroids. (Adapted from Paper I)

4.1.2 Virtual sorting of heterospheroid model based on mixed-species tumour cells and PSCs

Although double staining of an epithelial cell specific marker together with other protein markers is helpful to study tumour/stroma crosstalk at the protein level in the human tumour-human stroma models, the process is very time consuming and complicated. The detection of mRNA expression levels in human tumour-human stroma heterospheroids has limitations, especially for genes that are expressed by both cell types. To overcome this limitation, we developed a novel co-culture model based on pancreatic tumour cells and PSCs from different species cell types (human/mouse). This allowed us to directly detect the cell-type specific gene expression from intact heterospheroids through species-specific primers for qRT-PCR, which were named "virtual sorting".

We first set up the human tumour cell Panc1 monospheroids and mouse PSC (imPSCc3) monospheroids, as well as Panc1/imPSCc3 heterospheroids. By virtual sorting of Panc1 and imPSCc3 mono- and heterospheroids, we demonstrated the activation of imPSCc3 in heterospheroids with higher expression levels of *Acta2*, *Col1a1*, *Fn1* and *Tgfb1* compared to monospheroids (Fig.10 A). Furthermore, a higher expression level of *MKI67* and a lower expression level of *CDH1* were detected in Panc1 from heterospheroids compared to monospheroids (Fig.10B). To further verify the versatility of the heterospecies heterospheroids system, we also co-cultured the mouse tumour cells, KPCT, with human PSCs. Virtual sorting results also showed that the hPSCs were activated by the co-cultured KPCT, indicated by increased expression of *ACTA2*, *COL1A1*, *FN1* and *TGFB1* in hPSC from heterospheroids compared to monospheroids (Fig.10C).

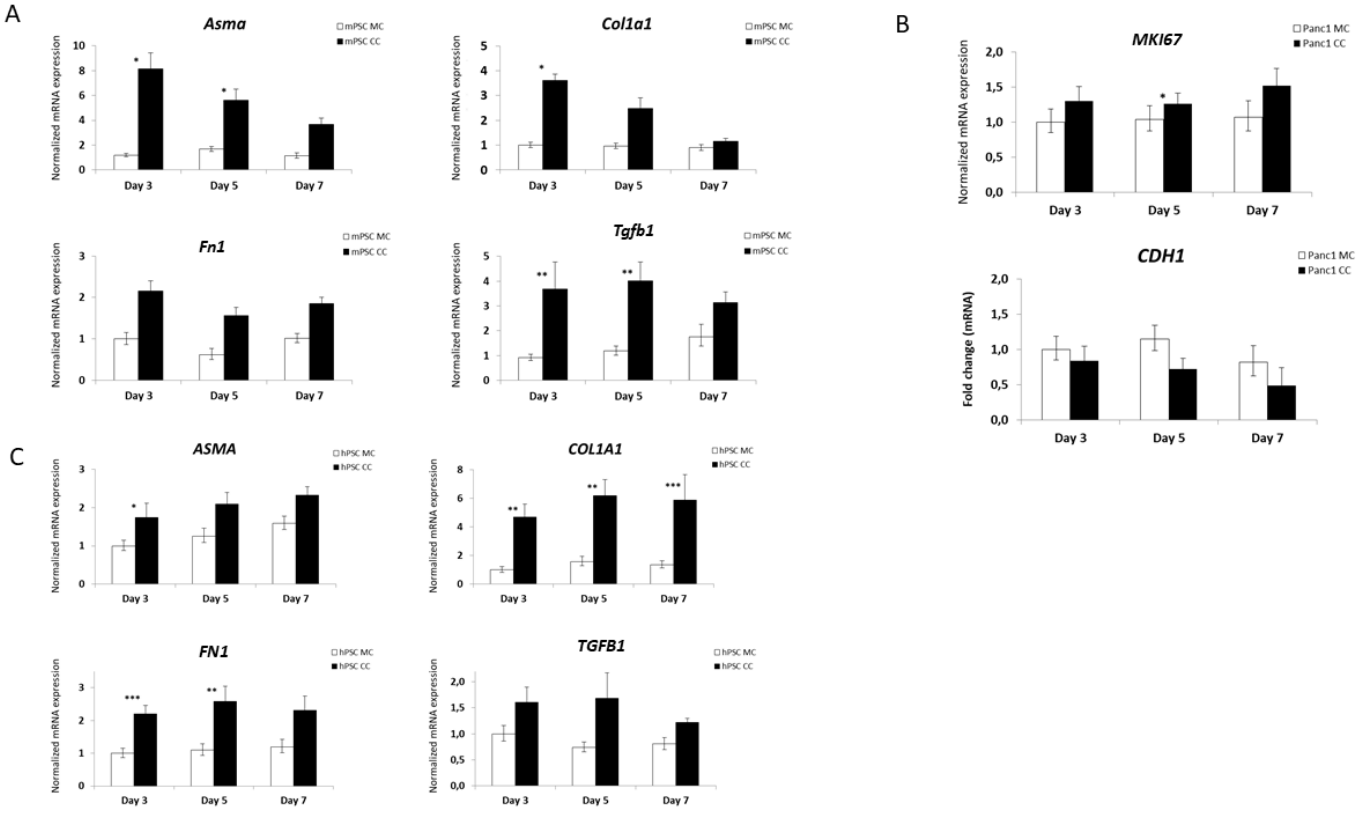

Fig.10 (A) Normalized mRNA expressions of *Asma* (*Acta2*), *Fn1*, *Col1a1* and *Tgfb1* in mPSCs from monospheroids and heterospheroids. (B) Normalized mRNA expressions of *MKI67* and *CDH1* in Panc1 from monospheroids and heterospheroids. (C) Normalized mRNA expressions of *ASMA* (*ACTA2*), *FN1*, *COL1A1* and *TGFB1* in hPSCs from monospheroids and heterospheroids. MC, monospheroids; CC, heterospheroids. (Adapted from Paper I)

4.2 Paper II

4.2.1 The characterisation of Panc1/mPSCs heterospecies heterospheroids at the global transcriptional level indicated hallmarks of PDAC

To expand the detection of pancreatic tumour/stroma crosstalk to a global level, we did the bulk RNA-seq of Panc1 and mPSCs mono- and heterospheroids. A series of software packages were used to separate the reads from the mixed libraries of Panc1 and mPSCs *in silico*, followed by the comparison of the global transcript level changes between monospheroids and heterospheroids for Panc1 and mPSCs, individually.

Under high serum condition, the enriched gene sets related to cell cycle, DNA replication and EMT in Panc1 from heterospheroids compared to monospheroids were identified using GSEA (Fig.11A). The higher expression levels of the proliferation marker *MKI67*, and mesenchymal markers *VIM* and N-cadherin (*CDH2*) that were detected by qRT-PCR in Panc1 from heterospheroids compared to monospheroids supported these GSEA results (Fig.11B). In addition, the gene sets describing ECM receptor interactions, lipid metabolism reprogramming (cholesterol homeostasis) and general

signalling pathways including MYC, mTORC1 and TNF/NF-κB were also enriched in Panc1 from heterospheroids compared to monospheroids (Fig.11A). For mPSCs under high serum condition, the gene sets related to hedgehog signalling, WNT β-catenin signalling and cell adhesion molecules were enriched in heterospheroids compared to monospheroids (Fig.11C). The expression level of *Gli1*, the effector of hedgehog signalling, was more than 100 times higher in mPSCs from heterospheroids compared to monospheroids based on qRT-PCR results (Fig.11D). On the other hand, the gene sets related to interferon alpha and -gamma (IFNα, -γ), MYC signalling, Toll like receptor signalling and proteasome were enriched in mPSCs from monospheroids compared to heterospheroids (Fig.11C).

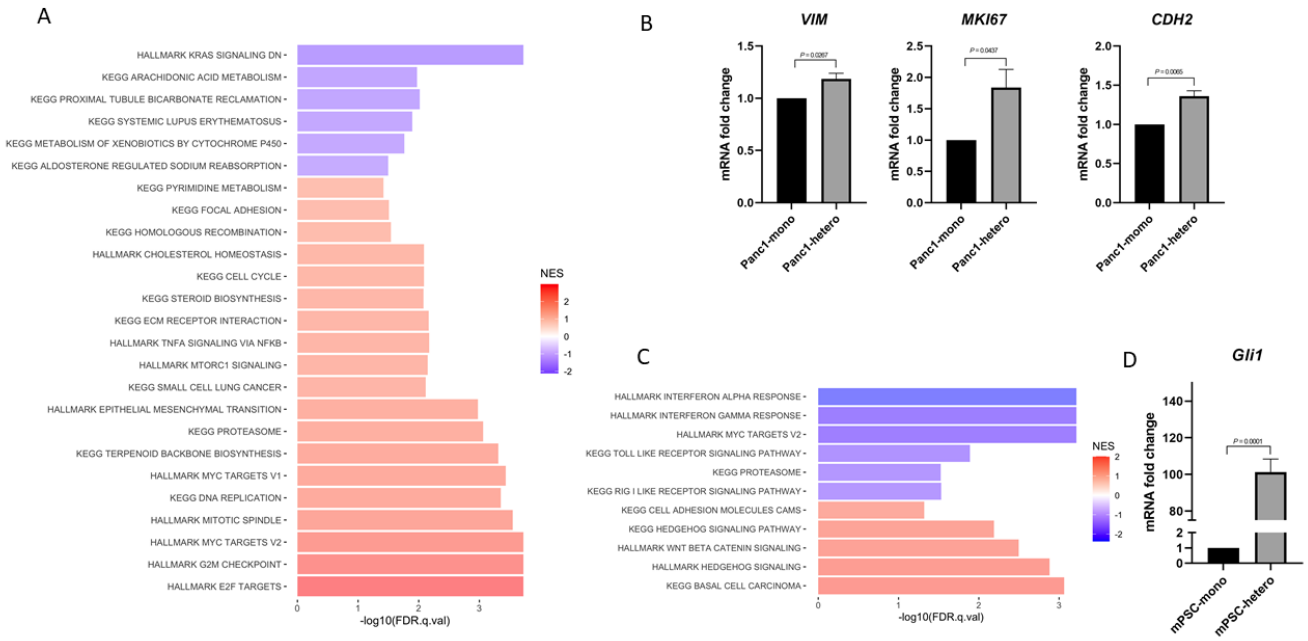

Fig.11 (A) The gene sets that were enriched in Panc1 from heterospheroids and monospheroids under high serum condition with FDR *q*-value < 0.05 by GSEA. (B) Normalized mRNA expressions of *VIM*, *MKI67* and *CDH2* in Panc1 from monospheroids and heterospheroids. (C) The gene sets that were enriched in mPSCs from heterospheroids and monospheroids under high serum condition with FDR *q*-value < 0.05 by GSEA. (D) Normalized mRNA expressions of *Gli1* in mPSCs from monospheroids and heterospheroids. (Adapted from Paper II)

Under low serum condition, the results of GSEA showed that the gene sets related to IFNα signalling, proteasome, EMT and TNF/NFκB signalling were enriched in Panc1 from heterospheroids compared to monospheroids (Fig.12A). The higher expression levels of *CDH2* and *FN1* in Panc1 from heterospheroids compared to monospheroids detected by qRT-PCR also supported the finding of the enriched gene set for EMT (Fig.12B). For mPSCs grown under low

serum condition, the GSEA results showed that gene sets for cell adhesion molecules, calcium signalling pathway, neuroactive ligand-receptor interaction, hedgehog signalling, and hypoxia were enriched in heterospheroids compared to monospheroids (Fig.12C). On the contrary, gene sets including DNA replication and repair, MYC target, and oxidative phosphorylation were enriched in mPSCs from monospheroids compared to heterospheroids (Fig.12C).

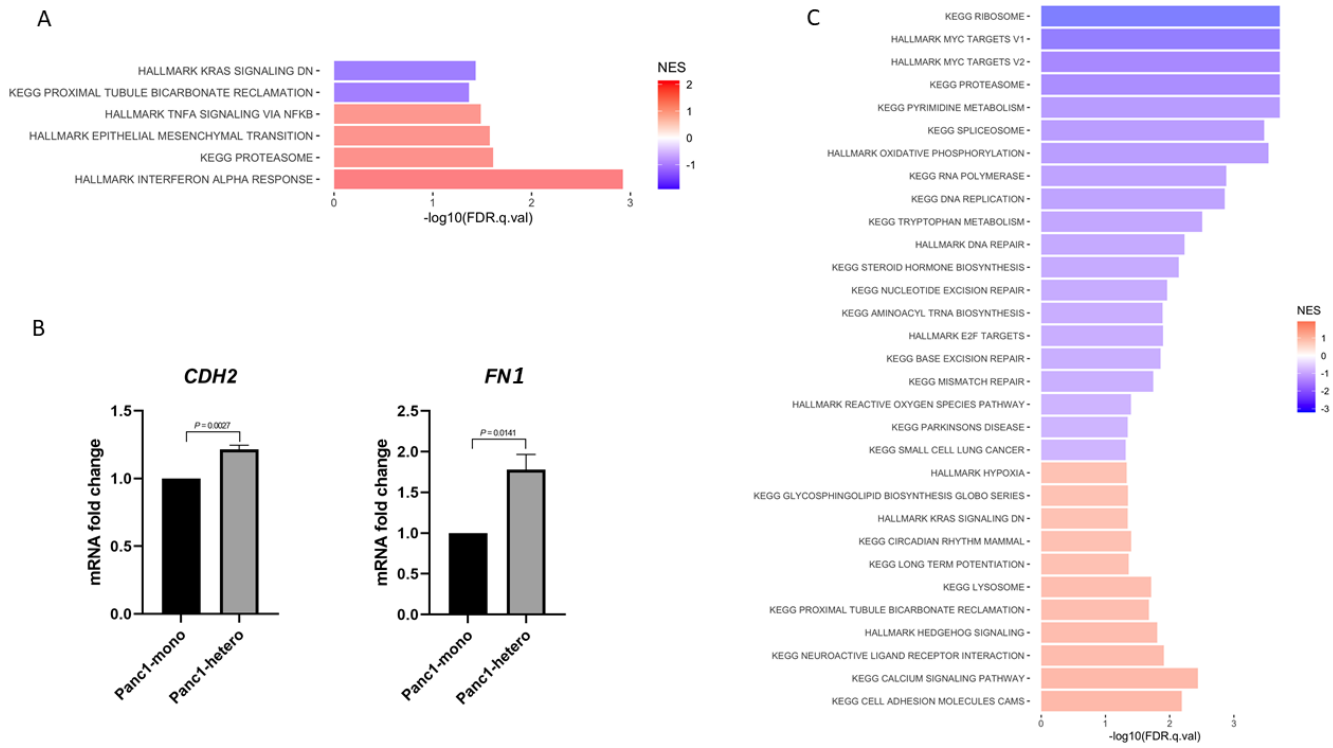

Fig.12 (A) The gene sets that were enriched in Panc1 from heterospheroids and monospheroids under low serum condition with FDR *q*-value < 0.05 by GSEA. (B) Normalized mRNA expressions of *CDH2* and *FN1* in Panc1 from monospheroids and heterospheroids. (C) The gene sets that were enriched in mPSCs from heterospheroids and monospheroids under low serum condition with FDR *q*-value < 0.05 by GSEA. (Adapted from Paper II)

4.2.2 Co-culture with mPSCs induced a phenotypical shift of Panc1 cells to a more aggressive molecular subtype of PDAC

By comparing DEGs of Panc1 (heterospheroids vs. monospheroids) grown under high serum condition to molecular signatures of PDAC, the basal-like/classical and squamous/progenitor, described by Moffitt et al.[30] and Bailey et al.[31], we found a significantly higher proportion of classical and progenitor signature genes with increased transcript levels in Panc1 from monospheroids (Fig.13A). However, a significantly higher proportion of basal-like and squamous signature genes with increased transcript levels were observed in Panc1 from heterospheroids (Fig.13A). Similarly, a higher proportion of progenitor and classical signature genes were enriched in Panc1 from monospheroids, while the squamous and basal-like signature genes were mostly

enriched in Panc1 from heterospheroids under low serum condition (Fig.13B). Therefore, Panc1 cells in monospheroids were more like progenitor/classical subtype, whereas Panc1 cells in heterospheroids were more reminiscent of squamous/basal-like subtype independent of culture conditions.

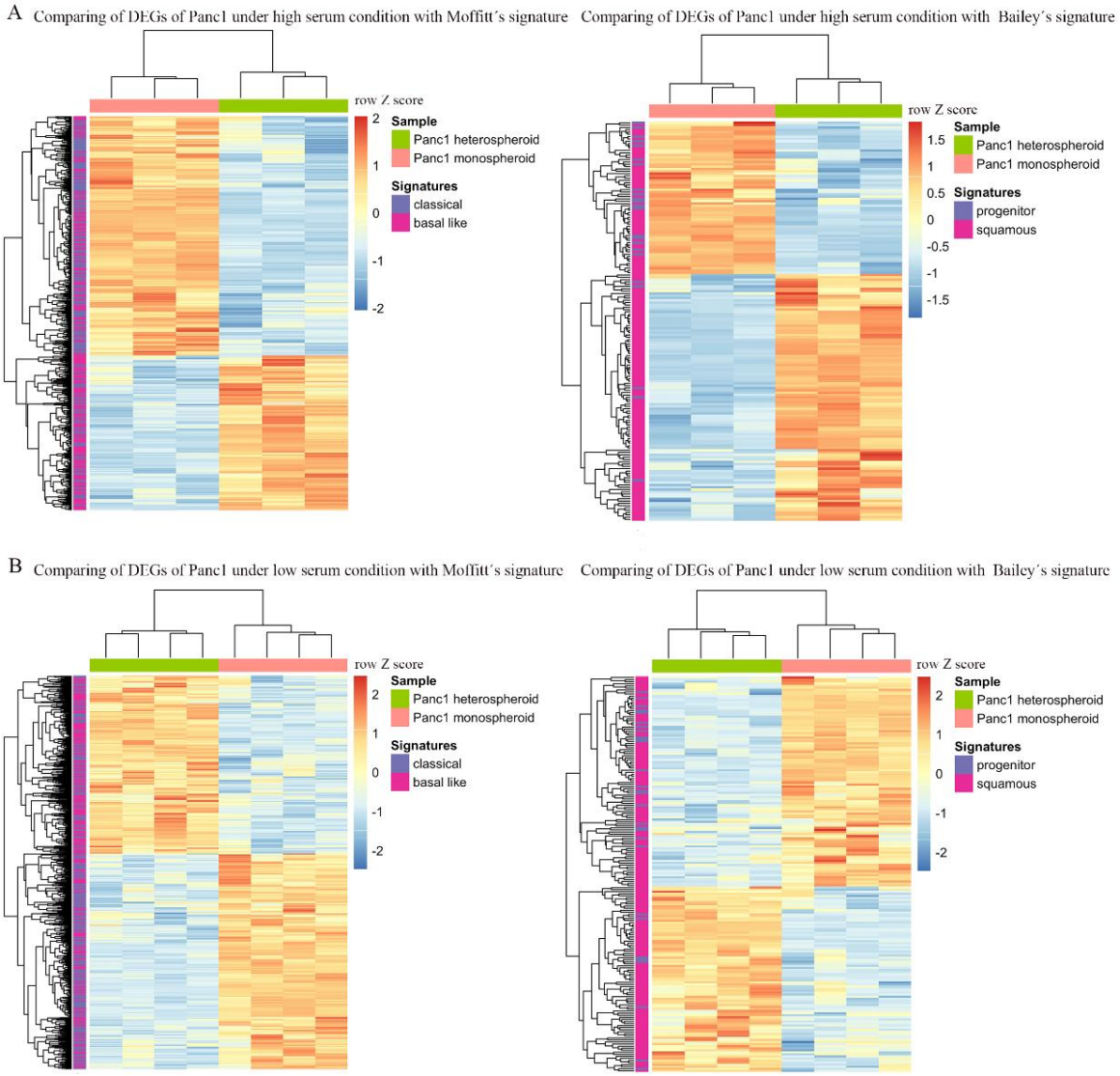

Fig.13 Heatmaps shows the comparison of DEGs from Panc1 (heterospheroids vs. monospheroids) under high (A) and low (B) serum condition to previously identified molecular signatures of the PDAC[30,31]. (Adapted from Paper II)

4.2.3 mPSCs acquired distinct CAF phenotypes induced by co-culture with tumour cells and the culture medium conditions

To investigate the possible heterogeneity of CAFs in our mPSCs spheroid model, we compared DEGs of mPSCs (heterospheroids vs. monospheroids) to the published myCAF and iCAF signature genes[38]. Under high serum condition, there was a trend of a higher proportion towards myCAF

signature genes with increased transcript levels in mPSCs from heterospheroids, whereas a larger proportion of iCAF signature genes with higher expression levels in mPSCs from monospheroids (Fig.14A). Using qRT-PCR, we further verified that significantly higher expression levels of iCAF marker genes *Il6*, *Il1r1* and *Cxcl1* were detected in mPSCs from monospheroids, while mPSCs from heterospheroids had significantly higher expression levels of myCAF markers *Acta2* and connective tissue growth factor (*Ctgf)* (Fig.14B). Unexpectedly, under low serum condition, there was a significantly higher proportion of iCAF signature genes enriched in mPSCs from heterospheroids, whereas a higher proportion of myCAF signature genes was enriched in mPSCs from monospheroids (Fig.14C). The qRT-PCR results showed that the expression levels of iCAF markers *Il6* and *Il1r1* were significantly higher in mPSCs from heterospheroids compared to monospheroids under low serum condition, corroborating the bioinformatics result (Fig.14D). However, under low serum condition, mPSCs from heterospheroids had also high expression levels of the myCAF markers *Cgtf* and *Acta2* compared to mPSCs from monospheroids (Fig.14D).

A previous study showed that TGFB signalling promoted the myCAF and counteracted the iCAF phenotype differentiation[70]. In our RNA-seq profiling, we also discovered an increased expression level of *Tgfb1* in mPSCs from heterospheroids compared to monospheroids under high serum conditions. To test whether the myCAF like phenotype of mPSCs from heterospheroids was induced by Tgfb1 signalling, we incubated Panc1/mPSCs heterospheroids cultured under high serum condition with TGFBR1/2 kinase inhibitor [5 µM] on day 1 for 72 hours. The qRT-PCR results showed that the expression of myCAF markers *Ctgf* and *Acta2* decreased, while the iCAF markers *Cxcl1* and *Il1r1* increased, indicating that blocking of Tgfb1 signalling shifted mPSCs from a more myCAF like subtype to a more iCAF like subtype (Fig.14E).

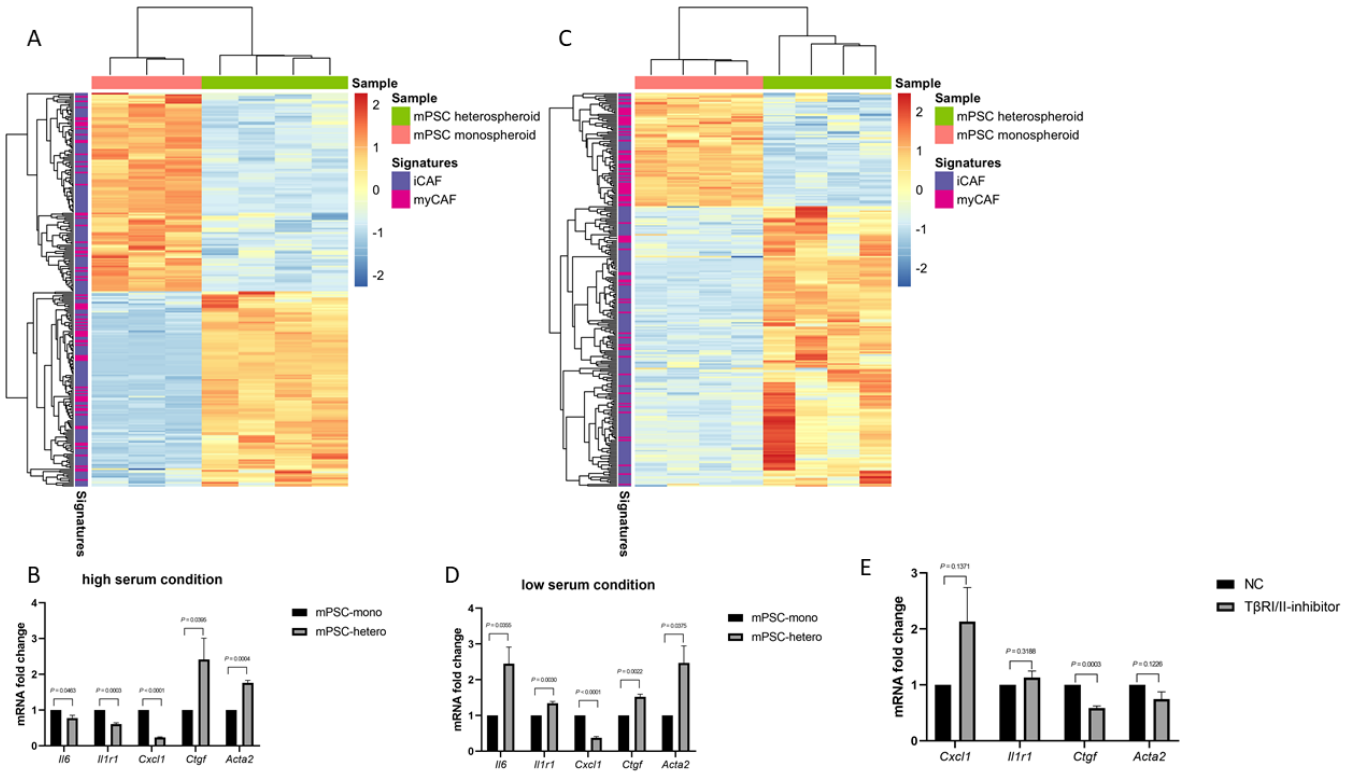

Fig.14 (A) Heatmap shows the comparison of DEGs from mPSCs (heterospheroids vs. monospheroids) under high serum condition to previously identified signatures of CAFs[38]. (B) Normalized mRNA expressions of myCAF and iCAF marker genes in mPSCs from monospheroids and heterospheroids under high serum condition. (C) Heatmaps show the comparison of DEGs from mPSCs (heterospheroids vs. monospheroids) under low serum condition to previously identified signatures of CAFs[38]. (D) Normalized mRNA expressions of myCAF and iCAF marker genes in mPSCs from monospheroids and heterospheroids under low serum condition. (E) Normalized mRNA expressions of myCAF and iCAF marker genes in mPSCs from heterospheroids under high serum condition treated with a TGFBR1/2 kinase inhibitor. (Adapted from Paper II)

4.2.4 mPSCs affected the chemosensitivity of Panc1 cells upon co-culture

To detect the influence of mPSCs on chemosensitivity of pancreatic tumour cells, we analysed the tumour cell specific apoptosis in Panc1 from heterospheroid and monospheroids using M30 Apoptosense® CK18 kit after treatment with the first-line chemotherapeutic drugs in PDAC patients. We found that Panc1 from heterospheroids had a significantly higher apoptosis rate compared to monospheroids after treatment with 50 µM gemcitabine under high serum condition (Fig.15A). In addition, we discovered higher expression levels of *SLC29A1* (solute carrier family 29 member 1 (augustine blood group), the major transporter of gemcitabine) and DCK (rate-limiting activating enzyme of gemcitabine) in Panc1 from heterospheroids compared to monospheroids by qRT-PCR (Fig.15B). However, Panc1 from heterospheroids had less apoptosis compared to monospheroids after treatment with paclitaxel [1 µM] and SN38 [1 µM] (Fig.15 C-D).

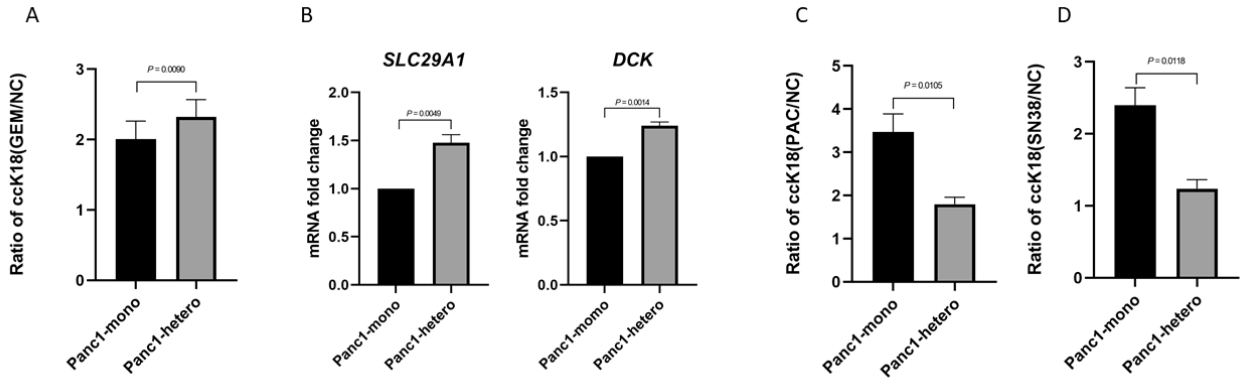

Fig.15 (A) The ratio of epithelial specific ccCK18 from Panc1 monospheroids and heterospheroids treated with 50 µM of gemcitabine. (B) Normalized mRNA expressions of *SLC29A1* and *DCK* in Panc1 from monospheroids and heterospheroids under high serum condition. (C-D) The ratio of epithelial specific ccCK18 from Panc1 monospheroids and heterospheroids treated with 1 µM of paclitaxel or SN38. PAC, Paclitaxel. (Adapted from Paper II)

4.2.5 Targeting cholesterol synthesis promoted apoptosis of Panc1 upon co-culture with mPSCs

As mentioned before, the cholesterol homeostasis gene set was enriched in Panc1 from heterospheroids compared to monospheroids under high serum condition (Fig.11A), which was supported by a higher expression level of 3-Hydroxy-3-Methylglutaryl-CoA Reductase (*HMGCR*), the rate-limiting enzyme for cholesterol synthesis, detected by qRT-PCR in Panc1 from heterospheroids compared to monospheroids under high serum condition (Fig.16A). To test whether targeting cholesterol synthesis could be a potential treatment for PDAC, we treated Panc1 monospheroids and Panc1/mPSCs heterospheroids with pitavastatin [5 μM] and detected a significantly higher apoptosis rate in Panc1 from heterospheroids compared to monospheroids (Fig.16B). In addition, pitavastatin treatment increased the expression of low-density lipoprotein receptor (*LDLR*) in Panc1 from both monospheroids and heterospheroids compared to NC (Fig.16C), while the absolute level of *LDLR* expression in Panc1 from heterospheroids and monospheroids were comparable independent of pitavastatin treatment. However, the expression level of proprotein convertase subtilisin/kexin type 9 (*PCSK9*) was considerably higher in Panc1 from heterospheroids compared to monospheroids after pitavastatin treatment (Fig.16D).

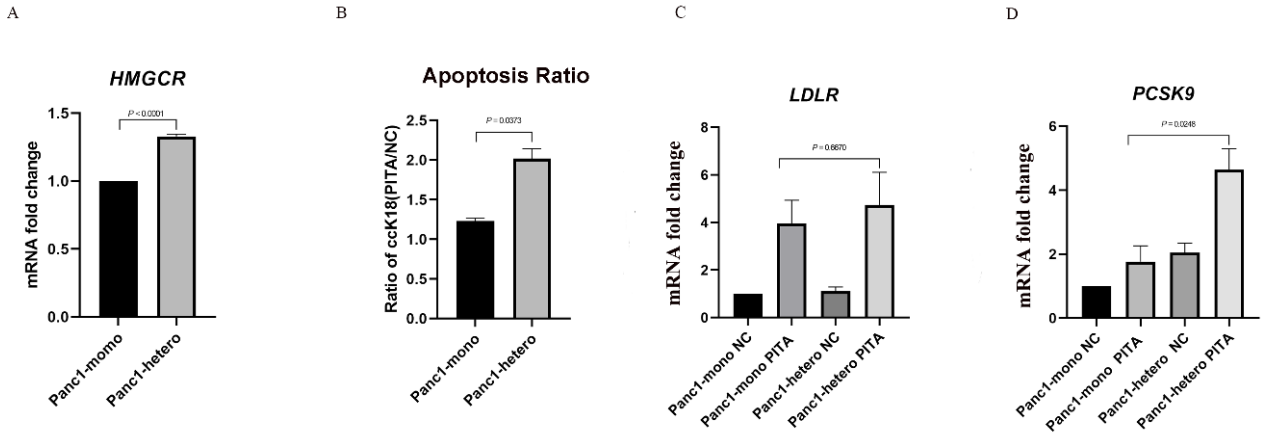

Fig.16 (A) Normalized mRNA expression of *HMGCR* in Panc1 from monospheroids and heterospheroids. (B) The ratio of epithelial-specific ccK18 from Panc1 monospheroids and heterospheroids treated with 5 μM of pitavastatin. (C-D) Normalized mRNA expressions of *LDLR* and *PCSK9* in Panc1 from monospheroids and heterospheroids treated with 5 μM of pitavastatin. (Adapted from Paper II)

4.3 Paper III

4.3.1 The expression level of CCN1 was increased in Panc1 cells upon co-culture with mPSCs.

In the RNA-seq profiling from Paper II, the *CCN1* expression level was significantly higher in Panc1 cells from heterospheroids compared to monospheroids, which was further verified by qRT-

PCR (Fig.17A). CRISPR-Cas9 technology was used to knockout *CCN1* in Panc1 cells, and three knockout clones C3, C7 and F3 were selected and verified by western blot (Fig.17B) and sanger sequencing.

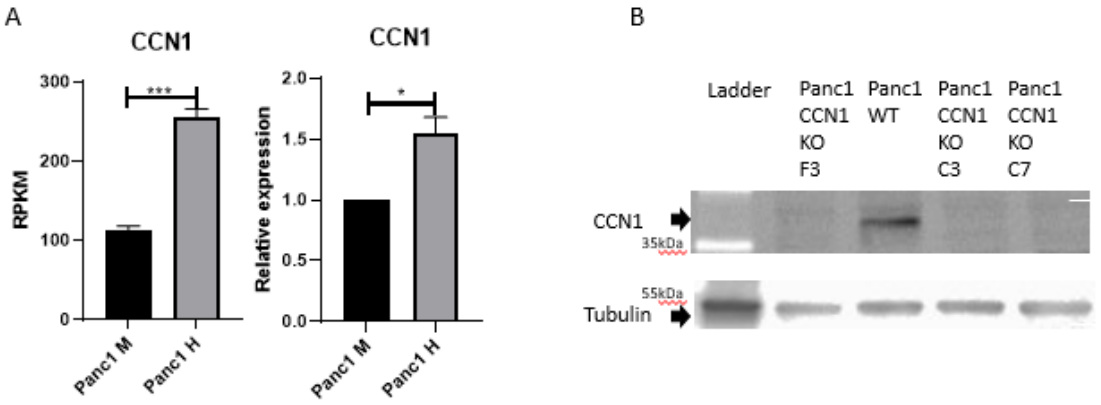

Fig.17 The expression level of *CCN1* in Panc1 from monospheroids and heterospheroids was analyzed by RNA-seq and qRT-PCR. (B) The representative western blot illustrates the expression of the CCN1 on protein level from Panc1-WT and 3 different Panc1-CCN1-KO clones (C3, C7 and F3) cultured in 2D. M, monospheroid; H, heterospheroid. (Adapted from Paper III)

4.3.2 CCN1 negatively modulated a stemness gene and positively regulated a gemcitabine transporter and - metabolising enzyme gene.

To examine functions related to CCN1, we analysed the mRNA expression of several genes in Panc1-CCN1-KO monospheroids versus unmanipulated/non-edited Panc1 control monospheroids. Panc1-CCN1-KO monospheroids had a significantly higher expression level of the stemness marker *CD24*, whereas lower expression levels of the epithelial markers *CK19* and *CDH1*, suggesting CCN1 may negatively regulate stemness/ affect cellular plasticity of Panc1 cells (Fig.18A). In addition, the expression levels of the gemcitabine transporter *SLC29A1* and the gemcitabine activating enzyme *DCK* were also lower in Panc1-CCN1-KO monospheroids compared to Panc1 control monospheroids (Fig.18A). The significantly decreased mRNA expression of *DCK* in Panc1-CCN1-KO cells was confirmed at the protein level by western blot (Fig.18B). We further detected a correlation between *CCN1* and its related genes by interrogating the publicly available microarray dataset GSE71729 of tumour samples from PDAC patients. The transcript level of *CCN1* was significantly inversely correlated to *CD24* but positively correlated with *DCK* expression, supporting the results obtained from our spheroid model (Fig.18C). Altogether, these results suggested that CCN1 might affect cellular plasticity (stemness and epithelial phenotype) and regulate gemcitabine sensitivity.

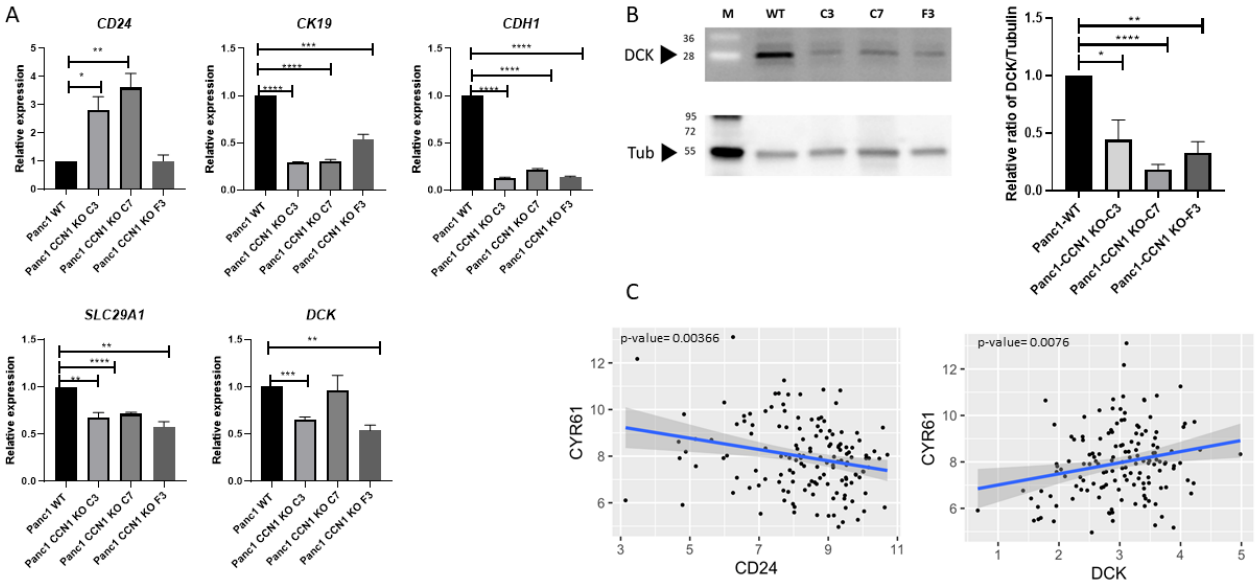

Fig.18 (A) Normalized mRNA expression levels of *CD24*, *CK19*, *CDH1*, *SLC29A1* and *DCK* in Panc1-WT and Panc1-CCN1-KO clones (C3, C7 and F3) from monospheroids. (B) The protein level of DCK in Panc1-WT and Panc1-CCN1-KO clones cultured in 2D. The relative ratio of DCK expression was quantified by DCK amount per lane / Tubulin amount per lane and then normalized to Panc1-WT. (C) The associations between *CCN1(CYR61)* and *CD24* and *DCK* based on the microarray dataset GSE71729. (Adapted from Paper III)

4.3.3 Lack of CCN1 impaired gemcitabine chemosensitivity

Since decreased expression levels of the key regulators of gemcitabine sensitivity, *SLC29A1* and *DCK*, were observed in Panc1-CCN1-KO monospheroids, we further examined the chemosensitivity towards gemcitabine in Panc1-CCN1-KO compared to Panc1 control cells. The results showed that gemcitabine induced growth inhibition was more effective in Panc1 control compared to Panc1-CCN1-KO cells in both classical monolayer culture and in monospheroids (Fig.19A). In addition, we also analysed gemcitabine induced apoptosis by detecting the epithelial specific ccCK18 in Panc1 control and Panc1-CCN1-KO cells from both monospheroids and heterospheroids. A lower apoptosis rate, indicated by a lower ccCK18 ratio of treated versus untreated, was observed in Panc1-CCN1-KO compared to Panc1 control monospheroids (Fig.19B). Furthermore, co-culturing with mPSCs increased gemcitabine-induced apoptosis for both Panc1 control and Panc1-CCN1-KO cells in heterospheroids (Fig.19B). On the other hand, no significant difference has been detected between Panc1 control and the Panc1-CCN1-KO cells for the ratio of ccCK18 from heterospheroid versus monospheroids (Fig.19C), suggesting that mPSCs may overexpress *Ccn1* to compensate the microenvironment for the missing expression of CCN1 when co-cultured with Panc1-CCN1-KO cells. Therefore, we analysed the expression of *Ccn1* in mPSCs

and found significantly increased *Ccn1* expression levels in mPSCs co-cultured with Panc1-CCN1-KO cells compared to Panc1 control cells (Fig.19D).

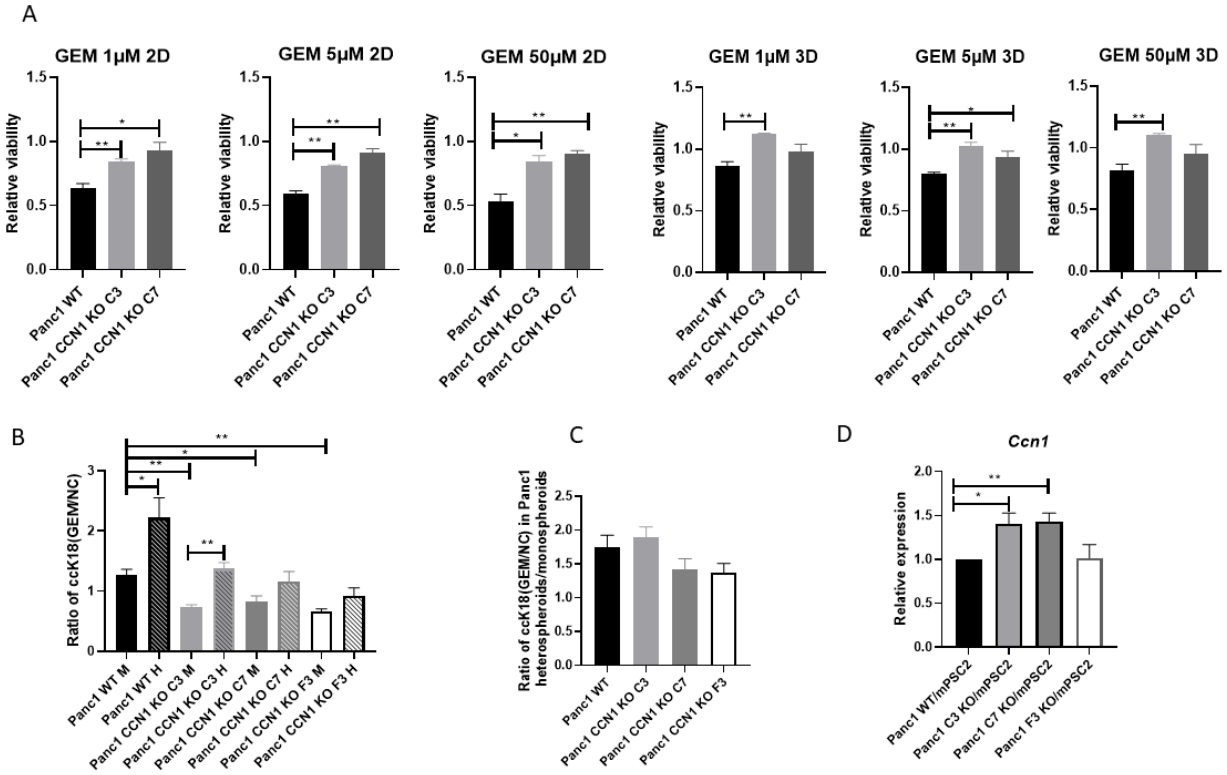

Fig.19 (A) The relative cell viability of Panc1 and Panc1-CCN1-KO cells treated with different doses of gemcitabine. (B) Ratios of epithelial specific ccCK18 for Panc1 and Panc1-CCN1-KO cells from monospheroids and heterospheroids treated with 50 μM of gemcitabine. (C) Relative ratios of ccCK18 for Panc1 control and Panc1-CCN1-KO from heterospheroids versus monospheroids. (D) mRNA expression of *Ccn1* in mPSCs from heterospheroids co-cultured with either Panc1 control or Panc1-CCN1-KO cells. (Adapted from Paper III)

4.3.4 LPA and TGFB1 upregulated the expression of *CCN1* in Panc1

It has been found that CCN1 is regulated by LPA and TGFB1 in breast cancer and prostatic epithelial cells[141,142]. In our spheroid models, we found that mPSCs in heterospheroids had increased expression levels of *Tgfb1* and *Enpp2* (ectonucleotide pyrophosphatase/phosphodiesterase family member 2). *Enpp2*, also named autotaxin, is a secreted enzyme converting lysophosphatidylcholine into LPA[55]. Therefore, we hypothesized that TGFB1 and LPA might also regulate CCN1 expression in pancreatic cancer cells. By stimulating Panc1 monospheroids with 20 μM of LPA under low serum condition (to minimize effects of phospholipids in FBS), we found significantly increased expression levels of *CCN1* and its downstream genes *CTGF* and *ITGA5*, as well as the proliferation marker *MKI67* (Fig.20A). Stimulation of Panc1 monospheroids grown under low serum condition (reducing influence of serum TGFB1 and LPA) with 5 μg/ mL recombinant TGFB1 protein also significantly increased the expression of *CTGF* and *ITGA5*, but the expression levels of *CCN1* and *MKI67* were affected in a statistically non-significant way (Fig.20A). Notably, stimulation of Panc1

monospheroids cultured under high serum condition with TGFB1 protein significantly increased *CCN1* as well as its downstream genes *CTGF* and *ITGA5* expression (Fig.20B). To further verify the regulatory mechanism of LPA and TGFB1 on *CCN1* expression, we blocked LPA and TGFB1 pathways by the autotaxin inhibitor PF8380 [10 μM] and the TGFB receptor kinase inhibitor LY2109761 [5 ng/mL] in Panc1/mPSCs heterospheroids grown under high serum condition on day 5, the time point when increased expression of *CCN1* was detected in Panc1 from heterospheroid compared to monospheroids. The results showed that *CCN1* expression was slightly decreased by incubation with either PF8380 or TGFBRi compared to NC, while the combination of both inhibitors strongly and significantly reduced the *CCN1* expression in Panc1 cells from heterospheroids (Fig.20C). The analysis of the microarray dataset GSE71729 of pancreatic cancer patients also revealed a positive correlation between *CCN1* and *ENPP2*, as well as *TGFB1* expression (Fig.20D). To determine the possible source(s) of LPA and TGFB1, which upregulated *CCN1* expression in Panc1 from heterospheroids, we compared the expression of *ENPP2*/*Enpp2* and *TGFB1*/*Tgfb1* in Panc1 and mPSCs between heterospheroids and monospheroids from RNA-seq profiling performed in Paper II. Notably, the expression of *Enpp2* was almost exclusively restricted to mPSCs (Fig.20E) since the expression of *ENPP2* in Panc1 was not detectable by RNA-seq and qRT-PCR (data not shown). Although *TGFB1*/*Tgfb1* were expressed by both Panc1 and mPSCs monospheroids, the expression of *Tgfb1* in mPSCs from heterospheroids was significantly increased compared to monospheroids (Fig.20E). However, no difference of *TGFB1* expression was detected in Panc1 cells from heterospheroids and monospheroids (Fig.20E).

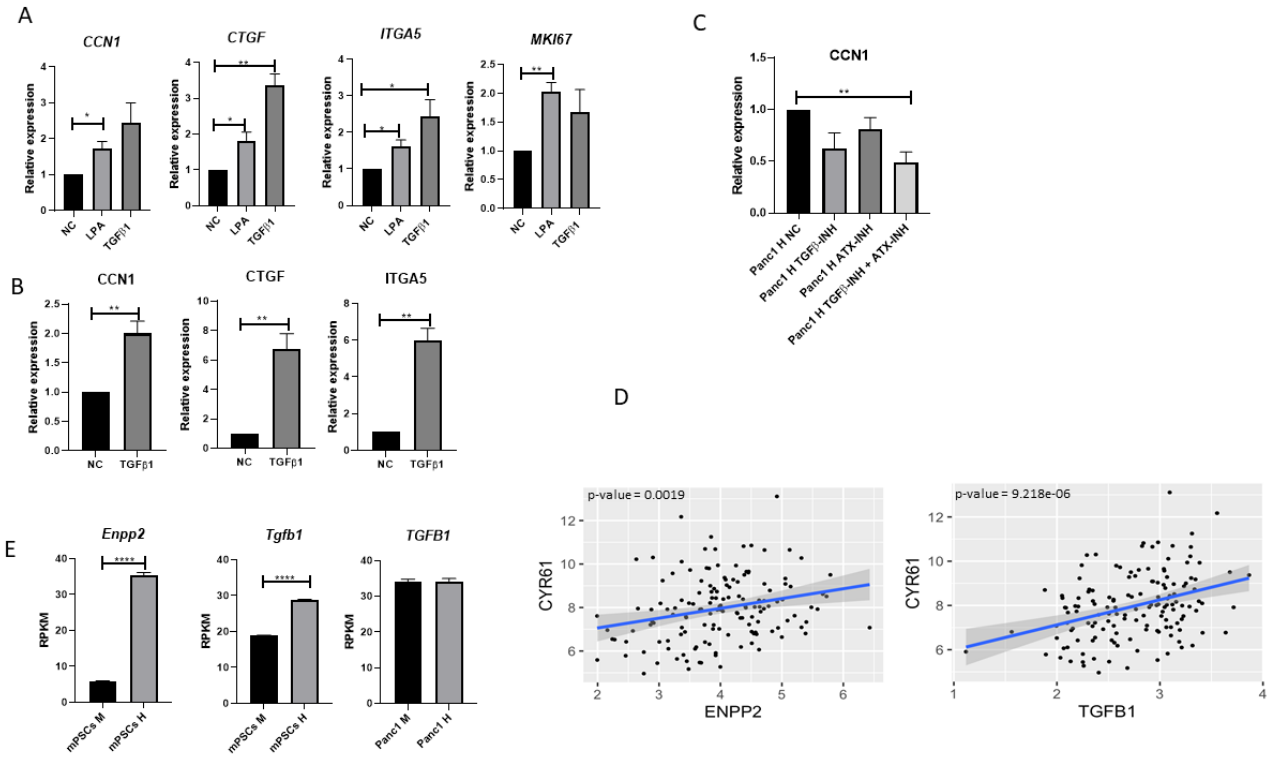

Fig.20 (A) mRNA expression of selected genes in Panc1 from monospheroids cultured under low serum condition stimulated with 20 μM of LPA or 5 μg/ mL of recombinant TGFB1. (B) mRNA expression of selected genes in Panc1 from monospheroids cultured under high serum condition

stimulated with 5 µg/ mL of recombinant TGFB1. (C) mRNA expressions of *CCN1* in Panc1 cells from heterospheroids stimulated with 5 ng/ mL of TGFB receptor kinase inhibitor or 10 µM of ATX/ Enpp2 inhibitor PF8380, or a combination of both inhibitors. (D) Associations between *ENPP2*, *TGFB1* and *CCN1* (*CYR61*) based on the microarray dataset GSE71729. (E) Expression levels of *Enpp2*, *Tgfb1* in mPSCs and *TGFB1* in Panc1 from monospheroids and heterospheroids. (Adapted from Paper III)

4.3.5 LPA and TGFB1 shifted mPSC to the more myCAF like subtype.

We further explored whether LPA and TGFB1 also regulated mPSCs. By stimulating mPSCs monospheroids with 5 µg/mL of recombinant human TGFB1, we found that the expression of *Ccn1* and the myCAF markers *Acta2*, *Ctgf*, as well as *Col1a1* were upregulated, but the iCAF marker *Cxcl1* was downregulated (Fig.21A). In addition, stimulation with 20 µM of LPA also significantly upregulated *Ccn1* expression but inhibited *Enpp2* expression in mPSCs from monospheroids (Fig.21B). Interestingly, LPA stimulation also upregulated the myCAF markers *Acta2* and *Ctgf* expression but downregulated the iCAF marker *Cxcl1* without affecting the expression of *Tgfb1*, suggesting LPA might be an additional mechanism to affect CAF subtypes (Fig.21B). For further validation, we blocked the LPA pathway in mPSCs/Panc1 heterospheroids by autotaxin inhibitor PF8380. As expected, the inhibitor significantly downregulated the expression of the myCAF markers *Acta2* and *Ctgf* (Fig.21C). In addition, the analysis of the microarray dataset GSE71729 derived from bulk PDAC tissue also showed a positive correlation between *ENPP2* and *ACTA2* expression (Fig.21D). Taken together, these findings indicated that both LPA and TGFB1 upregulated *Ccn1* expression in mPSCs and shifted mPSCs to a more myCAF-like phenotype.

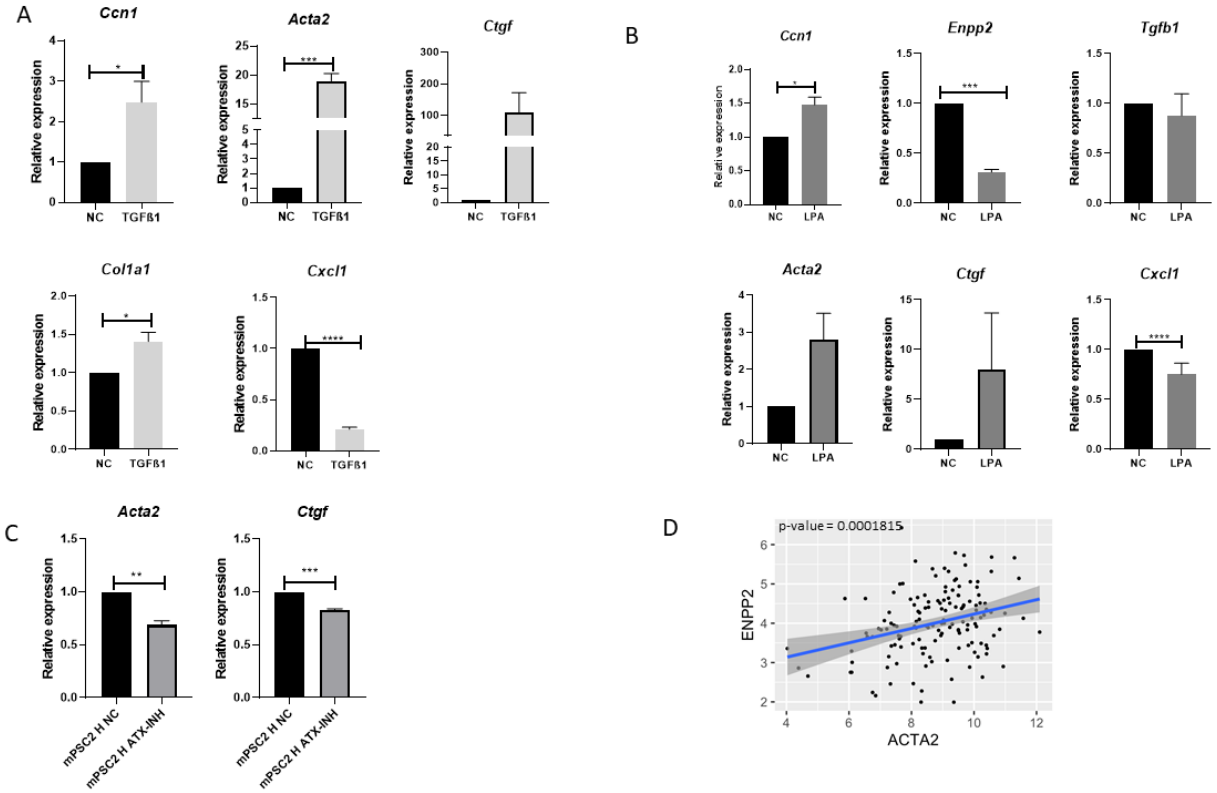

Fig.21 (A) mRNA expression of genes in mPSCs monospheroids stimulated with 5 μg/ mL recombinant of TGFB1. (B) mRNA expression of genes in mPSCs monospheroids stimulated with 20 μM of LPA. (C) mRNA expression of genes in mPSCs from heterospheroid stimulated with 10 μM of ATX/ Enpp2 inhibitor PF8380. (D) Associations between *ACTA2* and *ENPP2* based on the microarray dataset GSE71729. (Adapted from Paper III)

5 DISCUSSION

We firstly set up a scaffold-free and high reproducible 3D model by co-culturing different human pancreatic cancer cells (Panc1 and HPAFII) with immortalized human PSCs to study the tumour-stroma crosstalk. Notably, these two co-culture models using different tumour cells differed distinctly, including morphology and molecular features (e.g., VIM and CDH1). The reasons might lie in the different phenotypes of the two tumour cell lines, since the Panc1 cell line originated from the primary tumour tissue of the patient classified as a poorly differentiated grade 3 tumour[104]. The HPAFII cell line was derived from the peritoneal ascitic fluid of a patient with a moderately differentiated, grade 2 tumour[104]. Despite these differences, the increased proliferation of the tumour cells and the activation of PSC upon co-culture have been observed in both models, suggesting that some general reciprocal signalling between tumour cells and PSCs exists in pancreatic cancer. Since Panc1 cells were reported with a more aggressive phenotype, it was chosen for further studies in paper II and paper III[104].

As CK19 antibodies specifically stained the human epithelial tumour cells (Panc1 and HPAFII) but not the hPSCs, it allowed to separate these two cell types in the co-culture models and determine other molecules in a cell type specific manner by co-staining with other antibodies, e.g. MKI67. However, the staining procedure was complicated and of low throughput, and serial sections of the spheroids were needed to reflect the whole picture of the model. In addition, detection of mRNA expression changes between monospheroids and heterospheroids in specific cell types was difficult in the human tumour and human stroma co-culture models. Our lab tried to analyse the gene expression levels of the different cell types from heterospheroids following dissociation into single cells and fluorescence activated cell sorting[128]. However, this method had very low efficiency. In addition, the long procedure of cell separation caused cellular stress that affected gene expression. Therefore, the virtual sorting method which determined cell type specific genes expression by species-specific primers without the need for a dissociation step was developed.

By using this "virtual sorting" method on heterospecies heterospheroids, we verified the results we observed from human-human heterospheroids, including the increased expression of MKI67 and decreased CDH1 in Panc1 cells from heterospheroids compared to monospheroids. The heterospecies heterospheroids made of human tumour-mouse PSC (Panc1-mPSCs) and mouse tumour-human PSC (KPCT-hPSCs) shared several common characteristics, e.g., both PSCs got activated upon co-culture with tumour cells, indicated by higher expression levels of the classical activation markers *ACTA2*/*Acta2*, *FN1*/*Fn1*, *COL1A1*/*Col1a1* and *TGFB1*/*Tgfb1* in heterospheroids compared to monospheroids, which further confirmed the results from pure human-human Panc1-hPSCs co-culture model. Taken together, these expression changes between heterospheroids and monospheroids were clear evidence for tumour-stroma crosstalk in our 3D models, and no major differences between mouse and human PSCs were detected, paving the way to study tumour-stroma interaction on a global level in the heterospecies heterospheroid model.

In paper II, we detected the gene expression changes between monospheroids and heterospheroids of Panc1 and mPSCs under both high serum and low serum conditions, which could mimick the high and low nutrient situations in PDAC. Under high serum condition, the genes with higher expression levels in Panc1 from heterospheroids compared to monospheroids enriched in the pathways that reflected the main hallmarks of PDAC, including proliferation, EMT, ECM receptor interaction, focal adhesion and cholesterol homeostasis. On the other hand, the inflammation-related pathways of IFNα and TNFα-NFκB were enriched in Panc1 from heterospheroids compared to monospheroids when cultured under low serum condition. The difference in enriched pathways between high serum and low serum condition support the idea that the tumour biological processes are clearly affected by the nutrient condition in the TME.

The two major transcriptional subtypes of PDAC, classical/progenitor and basal-like/squamous, were first detected based on pancreatic cancer patients' tissues[30,31]. It was later found that the distinct transcriptional/expression signatures/phenotypes were driven by different genomic events, e.g. SMAD4 and GATA6 alterations were more associated with the classical subtype, while complete loss of CDKN2A and TP53 mutations were more related to the basal-like subtype[34]. In our study, we observed that paracrine communication between pancreatic tumour cells and PSCs promoted subtype transition, highlighting the roles of the TME in tumour subtype classification. Our finding was confirmed by an *in vivo* study of two xenograft models: the orthotopically grafted organoid (OGO) model and the intra-ductally grafted organoid (IGO) model[143]. The main difference between the two models was the TME surrounding the tumour cells: the IGO transplants were engrafted in the pancreatic ducts, while the OGO transplants were exposed to the stroma components (including the PSCs) in the pancreas[143]. They found that the OGO xenografts were more like the basal-like PDAC, while IGO tumours were more like the classical subtype, suggesting that the stroma shifted tumour cells to a more aggressive phenotype[143]. In addition, they also observed that the EMT and interferon-α/γ response pathways were enriched in OGO tumours compared to the IGO xenografts, which was consistent with the GSEA result from our heterospheroid model cultured under the nutrient-poor condition[143]. Moreover, we also discovered that the two major subtypes, reflected by Panc1 from monospheroids and heterospheroids, seemed in a continuum that could interconvert from one to another. A scRNA-seq analysis based on an *in vitro* co-culture system also showed that CAFs shifted a patient-derived PDAC cell line to a more EMT-like and proliferative phenotype[53], supporting that subtypes of PDAC are influenced by the TME. The mechanisms of molecular subtype plasticity of PDAC are still under study. The activation of MYC and TP63 transcriptional factors and the EMT process have been found to drive the basal-like subtype[144,145]. Since Panc1 cells from heterospheroids had significant enrichment of the MYC pathway and did not express TP63, we hypothesized that the MYC signalling might drive the shifting of Panc1 cells to a basal-like subtype in our spheroid model.

The preliminary pre-clinical and clinical data suggested tumours with distinct subtypes might respond differently to the first-line chemotherapy drug-combo of FOLFIRINOX and gemcitabine plus nab-

paclitaxel[146]. Collision et al. discovered that the quasi-mesenchymal cell lines were more sensitive to gemcitabine compared to the classical ones[29]. Furthermore, early results from the "Comprehensive Molecular Characterisation of Advanced Pancreatic Ductal Adenocarcinoma for Better Treatment Selection" cohort heightened the potential sensitivity of basal-like tumours to gemcitabine-based regimens, and classical tumours had better outcomes with modified FOLFIRINOX treatment[147]. Besides, Porter et al. also observed that patient-derived cell lines with classical epithelial-like subtype had higher sensitivity to FOLFIRNOX[148]. In line with the previous discoveries, we also observed Panc1, a pancreatic tumour cell line, responded differently to distinct chemotherapy drugs. Panc1 cells from the heterospheroids, more like the basal-like/mesenchymal subtype, were more sensitive to gemcitabine, while the more classical like Panc1 cells from monospheroids were more sensitive to paclitaxel and SN38. However, the mechanism behind the distinct chemosensitivities for different molecular subtypes of PDAC is still unknown. In this thesis, we considered the tumour subtypes together with the CAF subtypes to study their influence on chemosensitivity.

Several subtypes of CAFs with different functions have been detected in the PDAC microenvironment. By using *in vitro* PSC and PDAC organoid co-culture models as well as PDAC tissues from humans and KPC models, Öhlund et al. were the first to identify the tumour-adjacent myCAF (directly interacting with tumour cells) with tumour restraining functions and tumour-distal iCAF (interacting with tumour cells over distance by secretome) with tumour supporting functions, which were further verified by single-cell analyses on PDAC patient tissues[38,72]. Later, the possible mechanisms for these CAF subtypes differentiation were discovered by Biffi et al[70]. They showed that TGFB signalling promoted myCAF differentiation, whereas the NF-κB pathway induced iCAF generation[70]. Consistently, we observed similar subtypes of mPSCs existed in our heterospecies heterospheroid model by comparing the RNA profiling of mPSCs to the myCAF and iCAF signatures[38]. Under high serum condition, mPSCs acquired a more myCAF-like phenotype upon directly interacting with Panc1 cells, and a higher transcript level of *Tgfb1* was observed in mPSCs from heterospheroids. The myCAF phenotype of mPSCs could be abrogated by a TGFBR1/2 kinase inhibitor. At the same time, we were surprised to find that mPSCs achieved an iCAF-like phenotype upon direct co-culture with Panc1 under low serum condition, which was further supported by the enriched NF-κB pathway in Panc1 cells upon co-culture with mPSCs. In line with the RNA-seq result, qRT-PCR results showed the iCAF markers *Il6* and *Il1r1* were higher expressed in mPSCs from heterospheroids under low serum condition. On the other hand, the myCAF markers, *Cgtf* and *Acta2*, were also highly expressed by mPSCs from heterospheroids under low serum condition, indicating coexistence of two different CAF sub-populations or existence of a mixed subtype in the heterospheroids. In conclusion, our heterospecies heterospheroid model showed the cellular plasticity of immortalized mPSCs and illustrated that both human PDAC cells and culture conditions affected the phenotype of CAFs.

There is abundant evidence that CAFs facilitate both intrinsic and extrinsic chemoresistance in PDAC[58,149-151]. The dense desmoplasia has been found to act as a physical barrier or sink that limits

effective drug delivery[58,151]. On the other hand, the interaction between CAFs and tumour cells also impaires chemosensitivity, e.g. CAFs compromise gemcitabine-induced apoptosis in tumour cells through IL-1β-IL-1R/associated kinase-4 pathway[152]. In addition, researchers also discovered that CAFs protected tumour cells from gemcitabine toxicity by secretion of deoxycytidine and exosomes[149,153]. In contrast, we identified that the myCAF-like mPSCs sensitized co-cultured pancreatic tumour cells Panc1 to gemcitabine, probably through upregulation of the gemcitabine importer *SLC29A1* and the gemcitabine activating enzyme *DCK*. The discrepant results may be explained by the heterogeneity of CAFs/mPSCs used in different studies, e.g. primary versus established PSC cell lines versus nonpancreas-derived fibroblasts.

In paper III, we further examined the mechanism of increased gemcitabine sensitivity of tumour cells upon co-culture with PSCs and discovered that it is presumably caused by the *CCN1* gene, which was significantly increased in Panc1. This was indicated by increased gemcitabine resistance and lower expression levels of *SLC29A1* and *DCK* observed in Panc1-CCN1-KO clones. We further discovered that TGFB1 and LPA from mPSCs were possible sources for the upregulation of *CCN1* expression in Panc1. In addition, LPA and TGFB1 were also potential candidates for a phenotypical shift towards a myCAF-like phenotype. The early CAF-depletion studies either by blocking the SHH pathway or genetically targeting αSMA+ cells resulted in poor prognosis in PDAC[63,65]. Besides, ablation of Shh-dependent CAFs significantly decreased the αSMA+ CAF population in the background of the KPC mouse model, suggesting a functional association between Shh-dependent CAFs and αSMA+ CAFs[154]. We also observed significantly increased expression of *Gli1* (Shh-responsive gene) in myCAF like mPSCs upon co-culture with Panc1 under high serum condition. Therefore, we speculate that the failure in targeting Shh-dependent or αSMA-positive CAFs lies in the preferential deletion of the myCAF subpopulation, which is later discovered to possess tumour-suppressive functions. The discoveries described in our thesis work may add another puzzle piece to the heterogeneous functions of CAFs regarding chemosensitivity in PDAC.

Paradoxically, converse results, namely that CCN1 promoted gemcitabine resistance in PDAC, were discovered by other groups[87,91]. These contradictory results may be due to different experimental approaches such as different genetic manipulation methods, since other groups used lentiviral-based RNA interference (RNAi) or CRISPR-Cas9 editing technology to study the functions of CCN1[87,91]. The lentiviral-based genetic modification technology risks the induction of unknown genomic integration of the lentivirus, which can disrupt or increase gene expression by insertional mutagenesis[155]. Besides, the constitutive expression of the Cas9 enzyme may induce additional off-target genomic editing. Also the RNAi technology has high off-target risks and incomplete silencing effect[156]. To overcome these potential problems, we chose the lipofection based transfer of the CRISPR-Cas9 components, guaranteeing only transiently expression of Cas9 and minimal toxicity. Another reason for the controversial results may be caused by the cell line. As the cell line cultured *in vitro* evolves over time, the same cell line in different laboratories may differ considerably in its

properties. This is a non-neglectable limitation of using cell lines for biological studies, so clarification from more advanced models, e.g. *ex vivo* or *in vivo*, is needed.

The major advantage of the heterospecies heterospheroid model described in our study is that it allowes the detecting of the tumour biology stemming from tumour/stroma interaction without dissecting the heterogeneous spheroids into single-cell suspension and cell sorting, since the long and harsh disaggregation and cell sorting steps to separate tumour and stroma cells would affect gene expression[157]. Besides, our co-culture model is suitable for genetic manipulation as we have demonstrated with the CCN1-KO in specific cell types to study the function of a given protein. In addition, our scaffold-free spheroid model showes high reproducibility, and is compatible with imaging analysis and adaptable to high throughput analyses/drug screening.

Although the heterospecies heterospheroid model advances our understanding of tumour/stroma crosstalk, there are still some limitations. One of the disadvantages is the immortalized PSCs used in our study, which are artificially manipulated to continuously divide and may possess less relevant attributes or functions than primary cells[158,159]. However, the availability of primary PSCs is limited, since they sometimes do not survive *ex vivo* or only grow for a limited number of passages before they go into senescence[159]. Öhlund et al. discovered similar activated phenotypes between the primary PSCs and immortalized PSCs when co-culture with tumour organoids, suggesting the potential usefulness of immortalized PSCs in the co-culture study[38]. The fact that our heterospheroid model is based on cell types from different species has advantages and limitations at the same time. There are some signalling molecules that are species-specific and may restrict some of the interactions between human tumour and mouse stromal cells[160]. However, a study that compared global gene expressions demonstrated conserved tissue-specific expression patterns between both species[161]. In addition, we also confirmed the similarity between mouse PSCs and human PSCs when co-cultured with pancreatic tumour cells in Paper I.

6 CONCLUSIONS

The thesis uncovers novel insights into the interaction between tumour and stroma in pancreatic cancer by an advanced 3D co-culture model. Particularly, the paracrine signalling networks between PDAC cells and stroma affect transcriptional subtypes of tumour cells and PSCs/CAFs. Moreover, the myCAF like mPSCs sensitize PDAC cells to gemcitabine upon co-culture. The main conclusions of each paper are highlighted below:

We set up a novel 3D co-culture model of human tumour cells and human PSCs that reflected tumour/stroma crosstalk in PDAC. Furthermore, a heterospecies heterospheroids model based on different species of tumour cells and PSCs was developed, which allowed to study cell type specific gene expression without cell dissociation. **(Paper I)**

Transcriptional characterisation of heterospecies heterospheroids discovered key features of PDAC. Co-culture with mPSCs shifted the PDAC cells towards the more aggressive, basal-like, subtype. At the same time, mPSCs got activated and achieved distinct cancer-related phenotypes (iCAF/myCAF) under different culture conditions, which further affected the drug sensitivity of cancer cells. **(Paper II)**

The paracrine stimulation through TGFB1 and LPA between mPSCs and Panc1 cells shifted mPSCs to achieve a more myCAF-like subtype and upregulated the expression of *CCN1* in Panc1 cells. CCN1-KO in Panc1 cells resulted in dedifferentiation into a more progenitor-like state and the sensitivity towards gemcitabine was blunted. (**Paper III**)

7 POINTS OF PERSPECTIVE

Although molecular subtypes of PDAC have been well elucidated by both bulk RNA-seq and scRNA-seq, the administration of different chemotherapeutic regimens, FOLFIRINOX or gemcitabine/nab-paclitaxel, according to molecular subtypes for individual tumours/patients in the clinical reality is still in its infancy. O'Kane et al. found that patients with classical tumours may benefit more than basal-like subtype when treated with FOLFIRINOX[162]. In addition to the molecular subtypes, Tiriac et al. and Nicolle et al. revealed pharmacotranscriptomic expression signatures that could predict chemotherapy sensitivity for PDAC patients[137,163]. Management of rational therapeutic strategies for PDAC patients based on molecular subtypes and/or chemosensitivity signatures may achieve advanced clinical benefits. However, these promising developments still await confirmation by other research groups and/or thorough clinical studies. Besides, the CAF heterogeneity may also affect the chemosensitivity of tumour cells, since we found that the myCAF like mPSCs promoted gemcitabine sensitivity of PDAC cells. Along these lines, another study observed that PDAC patients with higher serum levels of IL-6 and IL-1β, the major iCAF markers, had poor responses to gemcitabine[164]. Considering both neoplastic molecular subtypes and CAF subtypes influence chemosensitivity, deeper knowledge of the specific associations between tumour and CAF subtypes is urgently needed. As bulk RNA-seq only reveals the sum of all signals from the mixed cell population, the scRNA-seq together with spatial transcriptome analysis on patients´ tissues from larger PDAC cohorts might be promising methods to clarify this complicated question.

Recently, the therapy regimens have also been found to influence tumour subtypes, e.g. enrichment of basal-like signature over classical signature was observed in PDAC cells after FOLFIRINOX treatment, probably through the selection effect (depletion of the more sensitive subtype) and/or due to tumour cell plasticity[148,165]. This might partly explain the acquired resistance in PDAC patients with chemotherapy. Therefore, evaluation of molecular subtypes after chemotherapeutic treatment is important, which could guide the application of an effective drug. As surgery is unavailable for advanced PADC patients and biopsy is an invasive method to obtain tissues for molecular subtypes detection, linking tissue based transcriptional molecular subtype classification to other non-invasive methods, like radiomics, to characterize PDAC patients may be promising in the future.

The origins of CAFs, especially the significant heterogeneity in their subtypes in pancreatic cancer are still under investigation. We and other labs found that iCAF and myCAF represented different states of activated PSCs and could interconvert between each other *in vitro*[38]. Recently another scRNA-seq study identified two fibroblast populations in normal mouse pancreas that might generate the myCAF and iCAF subtypes in the tumour by differentiation trajectories and pseudo-time analysis[166]. In addition, a mesothelial cell population in the normal pancreas has been found to express the apCAF signature[166]. Developing lineage tracing models to study the origin of CAFs is needed in future research.

Targeting CAFs in TME looks like a promising therapeutical approach for PDAC. Considering the tumour-suppressive roles of sub-populations of CAFs in PDAC, further studies might focus on detecting treatment strategies that specifically delete tumour-promoting CAFs (e.g. iCAF and apCAF), block their signalling, or convert/re-educate them into tumour-restraining CAFs.

8 ACKNOWLEDGEMENTS

In a blink of an eye, my PhD study is coming to the end. I would like to express my heartfelt gratitude to all the people in my life. Thanks a lot for all your help, and support that made my PhD journey such exciting.

Especially, to my principal supervisor **Rainer Heuchel**, thank you for your patience, trust, understanding and endless support during the past 4.5 years. Thank you for encouraging me to think critically and creatively in research as well as for teaching me the experimental skills. Thank you also for your help in improving my writing skills, you are so kind to correct my grammar error. Under your guidance, I transformed from a doctor to a researcher. When I had questions, no matter in academics or life, you always help me selflessly. Your broad knowledge and strict attitude towards science will always inspire me in the future. I am so lucky to have such a nice, kind, supervisor like you.

My co-supervisor **Matthias Löhr**. Thank you so much for bringing me to the "PaCaRes" family and giving me endless support and encouragement in both research and life! You always provide me valuable suggestions in my research from both scientific and clinical aspects. As a great clinician and scientist, your strict attitude towards work will always inspire me. Thanks for the annually "Pancreas" retreat and the afterword Christmas party, which was the most exciting part at the end of every year and made our research group like a real family!

My co-supervisor **Anthony Wright**. Thank you for sharing your great ideas in my PhD research and for valuable advice on my manuscripts. You are always nice to talk, and kind for help. Your positive attitude towards science and life will always inspire me.

My mentor **Ying Zhao**. Thank you for your encouragement and support! You are so kind, whenever I met difficulties, no matter in research and life, you gave me invaluable help and promising suggestions. Your warmness, generosity and optimism always influence me. Thank you also for organizing the journal club, it is a very good opportunity for me to broaden my views.

I am extremely grateful to Prof. **Jihui Jia** at Shandong University. Thank you for pointing the light in the dark days of my life. And thank you for all your kind help, endless support and encouragement. Words cannot express my deepest gratitude to you. Your kindness, wisdom, sense of responsibility and the big pattern will inspire me throughout my whole life.

My co-authors: **Gustav Arvidsson**, thank you for your great help in my research. You are the teacher who introduces me to the bioinformatics area. Thank you for sharing all your great ideas and knowledge. Whenever I had problems about the analysis and come to you, you always gave me kind help, even during your parental leave and preparation of the dissertation. I am so grateful for your help! **Xidan Li**, thank you for your kind help, endless support, and encouragement! The first time I met you was in China; you gave a lecture about bioinformatics. Your humorous speech explaining bioinformatics in a simple language impressed me deeply. It was so lucky to meet you again in

Sweden and had you in my research. Thank you also for the nice suggestions in my halftime rehearsal! **Jianping Liu,** thank you for your great help in performing the RNA-seq in my research and the nice suggestions in my manuscript. You are always nice to talk and kind for help. Thank you for sharing your experience and ideas for research and life.

My colleagues at PaCaRes Lab: **Salvo Nania** and **Jessica Norberg,** thank you for teaching me the experiments and sharing your experiences in research and life. **Xuan Li**, thank you for your great help during my application for PhD, and for your warm company and kind help in my PhD study. **Beate Gündel**, thank you for your warm accompany and a great help in my research, as well as your cakes, candies, chocolates, that make the lab comfortable as the home. **Veronika Engelsberger, Katharina Eiseler**, **Förderer Julia**, **Dawid Rutkowski** and **Martin Sundin**, thank you for your great help in the experiments and your ideas for the research as well as the nice talk during the lunch. I am so appreciative of all your contributions to my PhD study. **Maximilian Kordes**, **Pauline Jung**, **Wiktor Rutkowski**, **Xi Wei**, **Emre Iseri**, **Qiaoli Wang** and **Johannes Löhr**, thank you for all your warm accompany and endless support. **Monica Hagbok** and **Helene Jansson**, thank you for all your help and endless support during my PhD research!

Pancreas researchers: **Daniel Öhlund**, it was very nice to talk with you during all the meetings. Thank you for sharing your thought and experience and your suggestions in my research. **Helen Kaipe** and **Laia Gorchs**, thank you for sharing your ideas and experience, very helpful. **Dhifaf Sarhan**, thank you for the nice suggestions and discussion. **Tarja Schröder** and **Raoul Kuiper**, thank you for your help on immunohistochemistry. **Lars Haag**, thank you for your help in performing electron microscopy. **Yasmin Yu**, thank you for teaching me the hypoxia chamber.

My colleagues and friends in TRACK: **Rui He** and **Wenyi Zheng**, thank you for all the help during my PhD study. When I have any problems, no matter in life and research, you are the first people in my mind to ask for help, and you are always there, giving me endless support. I am so lucky to have you in my life and I see the best look of love on you two. Rui, you are my idol. Wenyi, you are my idol´s favourite. **Xiuming Liang** and **Qing Wang**, thank you for your great help during my application for PhD, and for your kind help and warm care in my PhD study. You are so warm-hearted, guiding me from Shandong to Stockholm. Best wishes also to your lovely girls **Domy** and **Amy**. **Qiang Wang**, thank you for your great help and care. I am so grateful to have you in the same department and for sharing your experiences with me. Best wishes also for **Zhen Zheng**. **Yun Du**, I am so grateful to meet such a kind girl, being my neighbour in lab and home. Thank you so much for accompanying me to the hospital and for so many unforgettable tours. You open the box of my life after the COVID-19. **Zheyu Niu,** thank you for your great help in my PhD research and your clinical view sight always inspires me. **Xia Wang**, I am so happy to have such a warm-hearted sister, thank you for your dabaozi, making me feel the home taste. Best wishes also to lovely **Yuanda Niu**. **Kim Olesen**, we met at the Mid-Autumn Festival party when I just arrived in

Sweden, and you were my first foreign friend. Thank you for your support and care in the lab, guidance in the gym and for looking for nice Chinese food together.

Moustapha Hassan, thank you for your constant encouragement and help. Especially during my "critical moment", you help me resolutely and calmly. I will never forget your support and kindness. Professor **Harvest Gu**, Thank you for your constant encouragement and warm help! On my first day at KFC, you bumped me at the entrance and showed me to my supervisor. You also gave me a lot of help in my PhD study. I am so appreciative to have such a kind, wise and warm-hearted teacher and friend. **Manuchehr Abedi-Valugerdi**, thank you for your help and support in my PhD, and it was so nice to talk with you. Thank you for sharing your exciting ideas. **Kathrin Reiser**, thank you for your help and for providing such a nice working environment! **Nicolas Tardif**, thank you for your help, support and sharing the ideas and suggestions. It was very nice to work together with you in the cell culture lab. **David Breniere-Letuffe**, **Qingyang Zhang**, **Amir Sohrabi**, **Laia Sadeghi**, **Dhanu Gupta**, **Guannan Zhou, Xiaoli Li**, **Yikai Yin**, **Ibrahim ElSerafi**, **Fadwa Benkessou**, **Risul Amin**, **Fangyi Long** and **Ziting Wang**: it was so nice to meet you guys and work together with you, making my PhD journey wonderful.

My friends at KI: **Yujiao Wu,** thanks for your great help during my PhD applications, you are so kind and warm-hearted, answering my questions and giving me suggestions. **Chuanyou Xia**, thanks for your great help during my PhD and PhD applications and for picking me up at the airport when I arrived in Stockholm. I am so grateful and lucky to know you. **Qingda Meng** and **Shanshan Xie**, thank you for your great help and care in both research and life. I am so happy to meet you at the beginning of my PhD and thank you for sharing your experiences with me, that were so helpful. **Zhenxiang Zhao**, thank you for your help and company, it is my lucky to have you, the old friend, together with me in Stockholm. **Stephan Haas**, thank you for your support and help! There were so many nice memories, e.g. the parties and Chinese foods, we had together. **Jinghua Wu**, I am grateful to have a fellow of Inner Mongolia, with familiar tones and culture, in Sweden. You brought me a lot of fun. **Haidong Yao,** thank you for your support and help, and it was very nice to have a conference together with you. Best wishes also to your family. **Shengyuan Zeng**, thank you for your support and for accompanying me on such wonderful tours, good memories. **Xi Chen,** thank you for your company for the course and the nice trips in Prague and Romme. **Chen Li**, thank you for helping me bring the staff from China and for your support during my PhD. Best wishes also to **Chengxi Sun**. **Ting Wang**, very nice to know such a gentle girl and thank you for sharing ideas about 3D culture. **Feifei Yan** and **Long Jiang**, thank you for all your support and the nice noodles in your family, and also for seeing the lovely cats virtually. **Dan Huang**, it is very nice to talk to such a winsome girl and thank you for sharing your experience with me. **Shifeng Lian**, a partner in the "keep eating" group, thanks for your company. **Can Cui,** you were always so warm-hearted. Thanks for your help and support during my PhD. **Lu Dai**, thank you for sharing your experience and inviting me to have dinner in your home. **Xiaolu Zhang**, thanks for your help during my PhD, it was so nice to

talk with you at the KI retreat dinner. Best wishes also for **Bingnan Li** and your lovely son. **Yaxuan Liu**, thanks for your help in my PhD, and it was very nice to have my first course together with you. **Jingya Yu**, thanks for your help with my PhD application and for inviting me to your graduation party, very fun. **Ping Chen**, thanks for your bioinformatics course and nice talks during the train. **Keyi Geng**, thanks for your great help and sharing your knowledge about bioinformatics. **Shixing Zheng** and **Dongli Liu**, thank you for the nice talk and for sharing your experience with me. **Kejia Hu**, **Dang Wei**, **Xinhe Mao, Weiwei Bian, Yuanyuan Zhang**, **Xiaotian Yuan**, **Liu Yang**, **Hao Shi**, **Chunlu Wang**, **Chenhong Lin**, **Jingru Yu**, **Xiaofei Ye**, **Yangjun Liu**, **Weiyingqi Cui**, **Wenyu Li** and **Jinming Han**, thanks for all your help and support. Great thanks to my dear friends in KI housing: **Qing Liu**, **Dandan Song**, **Anxiong Long**, **Yi Zhang**, **Yujie Zhang**, **Junjie Ma**, **Danyang Li**, **Xiaomeng Hu...** for your company. **Keying Zhu**, **Jieyu Wu**, **Jielu Liu**, **Liyan Lu**, **Zehuan Liao**, **Xueqi Li**, I was so grateful to have courses together with you, and you were so kind to share ideas and experiences. Thanks to my partners from Shandong University: **Linghua Kong**, **Xiangling Xing**, **Weiwei Cai**, **Jiwei Gao** and **Hua Chen**, your endless care warmed me in Sweden.

My friends in Sweden: **Sisi Huang**, you cared and supported me so much in Stockholm. You always gave me nice suggestions on my site. I am so grateful to have you in Sweden. Best wishes to your coming baby. **Jiang Yu**, it was so nice to have lunch together with you and you gave me great help encouragement and suggestions. **Jiaqi Liu**, my neighbour in lappis, thank you for the company and help, and it was a good memory you taught me about making the cake. **Jiahui Zhao**, I am so grateful for the wonderful tour with you in Helsinki. Thanks to my art lovers: **Jinxia Hao**, **XiaoJun Xu**, **Xinyue Mao**, **Xin Shen**, **Yijia Zhai**, **Xiru Zhang**, **Ran Xu**, **Ruyue Zhang**, **Anqi Wang**, **Xi Li**, **Shanshan Xie** for the wonderful performances together with you. Thanks to my polar light tour group: **Xiaowan Chen**, **Yang Liu**, **Yuezhen Huang** and **Rong Wang** for the amazing journey.

My friends in China: **Ke Wang**, thanks for your company, you always support and enlighten me. Thank you for passing the flower/happiness to me at your wedding virtually. **Hao Ren**, thank you for your endless care and support, as well as the nice trip to Yantai. **Hongmei Dai**, thank you for your encouragement and your passion always inspires me. **Huijun Li**, we met each other when we were in middle school. You accompanied me in every hard time I had. I am so grateful I have you. **Jiwei Wang** and **Ran Xu**, thank you so much for your help. I am so appreciative of your effort when my father was ill. Best wishes also to your families. **Jun Zhang**, my little sister, thank you for your care and support when I was in Shandong and Stockholm. **Lulu Zhang**, thank you for your help and encouragement when I prepared the IELTS. **Lin Wu**, thank you for your suggestions and encouragement for my PhD application. **Xiao Yu,** thank you for your great help in Shandong and introducing me to Lin.

Thanks for financial support from China Scholarship Council.

感谢亲人们的支持! 非常感谢我的姥爷,谢谢您的鼓励,让我坚定地来瑞典读博.

最后**特别感谢**我的母亲**刘子玉**女士以及我的父亲**刘建武**先生! 感谢你们从小对我的培养和教育,理解和包容,爱和鼓励! 爸爸妈妈我爱你们!

9 REFERENCES

1 The global, regional, and national burden of pancreatic cancer and its attributable risk factors in 195 countries and territories, 1990-2017: a systematic analysis for the Global Burden of Disease Study 2017. *The lancet. Gastroenterology & hepatology* **4**, 934-947, doi:10.1016/s2468-1253(19)30347-4 (2019).

2 Klein, A. P. Pancreatic cancer epidemiology: understanding the role of lifestyle and inherited risk factors. *Nature Reviews Gastroenterology & Hepatology* **18**, 493-502, doi:10.1038/s41575-021-00457-x (2021).

3 Siegel, R. L., Miller, K. D., Fuchs, H. E. & Jemal, A. Cancer statistics, 2022. *CA: A Cancer Journal for Clinicians* **72**, 7-33, doi:https://doi.org/10.3322/caac.21708 (2022).

4 Schizas, D. *et al.* Immunotherapy for pancreatic cancer: A 2020 update. *Cancer Treat Rev* **86**, 102016, doi:10.1016/j.ctrv.2020.102016 (2020).

5 Löhr, M. Is it possible to survive pancreatic cancer? *Nature Clinical Practice Gastroenterology & Hepatology* **3**, 236-237, doi:10.1038/ncpgasthep0469 (2006).

6 Zeng, S. *et al.* Chemoresistance in Pancreatic Cancer. *Int J Mol Sci* **20**, 4504, doi:10.3390/ijms20184504 (2019).

7 Rahib, L. *et al.* Projecting cancer incidence and deaths to 2030: the unexpected burden of thyroid, liver, and pancreas cancers in the United States. *Cancer Res* **74**, 2913-2921, doi:10.1158/0008-5472.CAN-14-0155 (2014).

8 Ferlay, J. A.-O. *et al.* Estimating the global cancer incidence and mortality in 2018: GLOBOCAN sources and methods. *Int J Cancer* **144**, 1941-1953, doi:10.1002/ijc.31937 (2019).

9 Fan, X. *et al.* Human oral microbiome and prospective risk for pancreatic cancer: a population-based nested case-control study. *Gut* **67**, 120-127, doi:10.1136/gutjnl-2016-312580 (2018).

10 Michaud, D. S. *et al.* Plasma antibodies to oral bacteria and risk of pancreatic cancer in a large European prospective cohort study. *Gut* **62**, 1764-1770, doi:10.1136/gutjnl-2012-303006 (2013).

11 Kasuga, A. *et al.* Molecular Features and Clinical Management of Hereditary Pancreatic Cancer Syndromes and Familial Pancreatic Cancer. *Int J Mol Sci* **23**, doi:10.3390/ijms23031205 (2022).

12 Park, W., Chawla, A. & O'Reilly, E. M. Pancreatic Cancer: A Review. *Jama* **326**, 851-862, doi:10.1001/jama.2021.13027 (2021).

13 Ren, B., Liu, X. & Suriawinata, A. A. Pancreatic Ductal Adenocarcinoma and Its Precursor Lesions: Histopathology, Cytopathology, and Molecular Pathology. *The American journal of pathology* **189**, 9-21, doi:10.1016/j.ajpath.2018.10.004 (2019).

14 Esposito, I., Konukiewitz, B., Schlitter, A. M. & Kloppel, G. Pathology of pancreatic ductal adenocarcinoma: facts, challenges and future developments. *World J Gastroenterol* **20**, 13833-13841, doi:10.3748/wjg.v20.i38.13833 (2014).

15 McGuigan, A. *et al.* Pancreatic cancer: A review of clinical diagnosis, epidemiology, treatment and outcomes. *World J Gastroenterol* **24**, 4846-4861, doi:10.3748/wjg.v24.i43.4846 (2018).

16 Haeberle, L. & Esposito, I. Pathology of pancreatic cancer. *Transl Gastroenterol Hepatol* **4**, 50-50, doi:10.21037/tgh.2019.06.02 (2019).

17 Bhosale, P. *et al.* Genetics of pancreatic cancer and implications for therapy. *Abdom Radiol (NY)* **43**, 404-414, doi:10.1007/s00261-017-1394-y (2018).

18 Hruban, R. H., Maitra, A. & Goggins, M. Update on pancreatic intraepithelial neoplasia. *Int J Clin Exp Pathol* **1**, 306-316 (2008).

19 Vincent, A., Herman, J., Schulick, R., Hruban, R. H. & Goggins, M. Pancreatic cancer. *Lancet* **378**, 607-620, doi:10.1016/S0140-6736(10)62307-0 (2011).

20 Mazur, P. K. & Siveke, J. T. Genetically engineered mouse models of pancreatic cancer: unravelling tumour biology and progressing translational oncology. *Gut* **61**, 1488-1500, doi:10.1136/gutjnl-2011-300756 (2012).

21 Mizrahi, J. D., Surana, R., Valle, J. W. & Shroff, R. T. Pancreatic cancer. *Lancet* **395**, 2008-2020, doi:10.1016/s0140-6736(20)30974-0 (2020).

22 Conroy, T. *et al.* FOLFIRINOX versus gemcitabine for metastatic pancreatic cancer. *N Engl J Med* **364**, 1817-1825, doi:10.1056/NEJMoa1011923 (2011).

23 Dell'Aquila, E. *et al.* Prognostic and predictive factors in pancreatic cancer. *Oncotarget* **11**, 924-941, doi:10.18632/oncotarget.27518 (2020).

24 Golan, T. *et al.* Maintenance Olaparib for Germline BRCA-Mutated Metastatic Pancreatic Cancer. *N Engl J Med* **381**, 317-327, doi:10.1056/NEJMoa1903387 (2019).

25 Drilon, A. *et al.* Efficacy of Larotrectinib in TRK Fusion-Positive Cancers in Adults and Children. *N Engl J Med* **378**, 731-739, doi:10.1056/NEJMoa1714448 (2018).

26 Jones, M. R. *et al.* NRG1 Gene Fusions Are Recurrent, Clinically Actionable Gene Rearrangements in KRAS Wild-Type Pancreatic Ductal Adenocarcinoma. *Clinical cancer research : an official journal of the American Association for Cancer Research* **25**, 4674-4681, doi:10.1158/1078-0432.Ccr-19-0191 (2019).

27 Marabelle, A. *et al.* Efficacy of Pembrolizumab in Patients With Noncolorectal High Microsatellite Instability/Mismatch Repair-Deficient Cancer: Results From the Phase II KEYNOTE-158 Study. *Journal of clinical oncology : official journal of the American Society of Clinical Oncology* **38**, 1-10, doi:10.1200/jco.19.02105 (2020).

28 Dauer, P., Nomura, A., Saluja, A. & Banerjee, S. Microenvironment in determining chemo-resistance in pancreatic cancer: Neighborhood matters. *Pancreatology* **17**, 7-12, doi:10.1016/j.pan.2016.12.010 (2017).

29 Collisson, E. A. *et al.* Subtypes of pancreatic ductal adenocarcinoma and their differing responses to therapy. *Nature medicine* **17**, 500-503, doi:10.1038/nm.2344 (2011).

30 Moffitt, R. A. *et al.* Virtual microdissection identifies distinct tumor- and stroma-specific subtypes of pancreatic ductal adenocarcinoma. *Nature Genetics* **47**, 1168-1178, doi:10.1038/ng.3398 (2015).

31 Bailey, P. *et al.* Genomic analyses identify molecular subtypes of pancreatic cancer. *Nature* **531**, 47-52, doi:10.1038/nature16965 (2016).

32 Collisson, E. A., Bailey, P., Chang, D. K. & Biankin, A. V. Molecular subtypes of pancreatic cancer. *Nature Reviews Gastroenterology & Hepatology* **16**, 207-220, doi:10.1038/s41575-019-0109-y (2019).

33 Puleo, F. *et al.* Stratification of Pancreatic Ductal Adenocarcinomas Based on Tumor and Microenvironment Features. *Gastroenterology* **155**, 1999-2013 e1993, doi:10.1053/j.gastro.2018.08.033 (2018).

34 Chan-Seng-Yue, M. *et al.* Transcription phenotypes of pancreatic cancer are driven by genomic events during tumor evolution. *Nat Genet* **52**, 231-240, doi:10.1038/s41588-019-0566-9 (2020).

35 Collisson, E. A., Bailey, P., Chang, D. K. & Biankin, A. V. Molecular subtypes of pancreatic cancer. *Nature reviews. Gastroenterology & hepatology* **16**, 207-220, doi:10.1038/s41575-019-0109-y (2019).

36 Sun, Q. *et al.* The impact of cancer-associated fibroblasts on major hallmarks of pancreatic cancer. *Theranostics* **8**, 5072-5087, doi:10.7150/thno.26546 (2018).

37 Whiteside, T. L. The tumor microenvironment and its role in promoting tumor growth. *Oncogene* **27**, 5904-5912, doi:10.1038/onc.2008.271 (2008).

38 Öhlund, D. *et al.* Distinct populations of inflammatory fibroblasts and myofibroblasts in pancreatic cancer. *The Journal of experimental medicine* **214**, 579-596, doi:10.1084/jem.20162024 (2017).

39 Duffy, J. P., Eibl, G., Reber, H. A. & Hines, O. J. Influence of hypoxia and neoangiogenesis on the growth of pancreatic cancer. *Molecular Cancer* **2**, 12, doi:10.1186/1476-4598-2-12 (2003).

40 Kamphorst, J. J. *et al.* Human pancreatic cancer tumors are nutrient poor and tumor cells actively scavenge extracellular protein. *Cancer research* **75**, 544-553, doi:10.1158/0008-5472.CAN-14-2211 (2015).

41 von Ahrens, D., Bhagat, T. D., Nagrath, D., Maitra, A. & Verma, A. The role of stromal cancer-associated fibroblasts in pancreatic cancer. *Journal of hematology & oncology* **10**, 76, doi:10.1186/s13045-017-0448-5 (2017).

42 Dvorak, H. F. Tumors: wounds that do not heal-redux. *Cancer immunology research* **3**, 1-11, doi:10.1158/2326-6066.Cir-14-0209 (2015).

43 Arina, A. *et al.* Tumor-associated fibroblasts predominantly come from local and not circulating precursors. *Proceedings of the National Academy of Sciences of the United States of America* **113**, 7551-7556, doi:10.1073/pnas.1600363113 (2016).

44 Vaish, U., Jain, T., Are, A. C. & Dudeja, V. Cancer-Associated Fibroblasts in Pancreatic Ductal Adenocarcinoma: An Update on Heterogeneity and Therapeutic Targeting. *Int J Mol Sci* **22**, 13408, doi:10.3390/ijms222413408 (2021).

45 Pereira, B. A. *et al.* CAF Subpopulations: A New Reservoir of Stromal Targets in Pancreatic Cancer. *Trends Cancer* **5**, 724-741, doi:10.1016/j.trecan.2019.09.010 (2019).

46 Erkan, M. *et al.* StellaTUM: current consensus and discussion on pancreatic stellate cell research. *Gut* **61**, 172-178, doi:10.1136/gutjnl-2011-301220 (2012).

47 Apte, M. V. *et al.* Periacinar stellate shaped cells in rat pancreas: identification, isolation, and culture. *Gut* **43**, 128-133, doi:10.1136/gut.43.1.128 (1998).

48 Allam, A. *et al.* Pancreatic stellate cells in pancreatic cancer: In focus. *Pancreatology* **17**, 514-522, doi:10.1016/j.pan.2017.05.390 (2017).

49 Zhan, H. X. *et al.* Crosstalk between stromal cells and cancer cells in pancreatic cancer: New insights into stromal biology. *Cancer letters* **392**, 83-93, doi:10.1016/j.canlet.2017.01.041 (2017).

50 Wu, Q. *et al.* Functions of pancreatic stellate cell-derived soluble factors in the microenvironment of pancreatic ductal carcinoma. *Oncotarget* **8**, 102721-102738, doi:10.18632/oncotarget.21970 (2017).

51 Tape, C. J. *et al.* Oncogenic KRAS Regulates Tumor Cell Signaling via Stromal Reciprocation. *Cell* **165**, 910-920, doi:10.1016/j.cell.2016.03.029 (2016).

52 Shi, Y. *et al.* Targeting LIF-mediated paracrine interaction for pancreatic cancer therapy and monitoring. *Nature* **569**, 131-135, doi:10.1038/s41586-019-1130-6 (2019).

53 Ligorio, M. *et al.* Stromal Microenvironment Shapes the Intratumoral Architecture of Pancreatic Cancer. *Cell* **178**, 160-175.e127, doi:10.1016/j.cell.2019.05.012 (2019).

54 Sousa, C. M. *et al.* Pancreatic stellate cells support tumour metabolism through autophagic alanine secretion. *Nature* **536**, 479-483, doi:10.1038/nature19084 (2016).

55 Auciello, F. R. *et al.* A Stromal Lysolipid-Autotaxin Signaling Axis Promotes Pancreatic Tumor Progression. *Cancer discovery* **9**, 617-627, doi:10.1158/2159-8290.Cd-18-1212 (2019).

56 Zhao, H. *et al.* Tumor microenvironment derived exosomes pleiotropically modulate cancer cell metabolism. *eLife* **5**, e10250, doi:10.7554/eLife.10250 (2016).

57 Dalin, S. *et al.* Deoxycytidine Release from Pancreatic Stellate Cells Promotes Gemcitabine Resistance. *Cancer Res* **79**, 5723-5733, doi:10.1158/0008-5472.Can-19-0960 (2019).

58 Hessmann, E. *et al.* Fibroblast drug scavenging increases intratumoural gemcitabine accumulation in murine pancreas cancer. *Gut* **67**, 497-507, doi:10.1136/gutjnl-2016-311954 (2018).

59 Feig, C. *et al.* Targeting CXCL12 from FAP-expressing carcinoma-associated fibroblasts synergizes with anti-PD-L1 immunotherapy in pancreatic cancer. *Proceedings of the National Academy of Sciences of the United States of America* **110**, 20212-20217, doi:10.1073/pnas.1320318110 (2013).

60 Mace, T. A. *et al.* Pancreatic cancer-associated stellate cells promote differentiation of myeloid-derived suppressor cells in a STAT3-dependent manner. *Cancer Res* **73**, 3007-3018, doi:10.1158/0008-5472.Can-12-4601 (2013).

61 De Monte, L. *et al.* Intratumor T helper type 2 cell infiltrate correlates with cancer-associated fibroblast thymic stromal lymphopoietin production and reduced survival in pancreatic cancer. *The Journal of experimental medicine* **208**, 469-478, doi:10.1084/jem.20101876 (2011).

62 Rhim, A. D. *et al.* Stromal elements act to restrain, rather than support, pancreatic ductal adenocarcinoma. *Cancer cell* **25**, 735-747, doi:10.1016/j.ccr.2014.04.021 (2014).

63 Lee, J. J. *et al.* Stromal response to Hedgehog signaling restrains pancreatic cancer progression. *Proceedings of the National Academy of Sciences of the United States of America* **111**, E3091-3100, doi:10.1073/pnas.1411679111 (2014).

64 Catenacci, D. V. *et al.* Randomized Phase Ib/II Study of Gemcitabine Plus Placebo or Vismodegib, a Hedgehog Pathway Inhibitor, in Patients With Metastatic Pancreatic Cancer. *Journal of clinical oncology : official journal of the American Society of Clinical Oncology* **33**, 4284-4292, doi:10.1200/jco.2015.62.8719 (2015).

65 Özdemir, B. C. *et al.* Depletion of Carcinoma-Associated Fibroblasts and Fibrosis Induces Immunosuppression and Accelerates Pancreas Cancer with Reduced Survival. *Cancer cell* **28**, 831-833, doi:10.1016/j.ccell.2015.11.002 (2015).

66 Chen, Y. *et al.* Type I collagen deletion in αSMA+ myofibroblasts augments immune suppression and accelerates progression of pancreatic cancer. *Cancer cell* **39**, 548-565.e546, doi:https://doi.org/10.1016/j.ccell.2021.02.007 (2021).

67 Bhattacharjee, S. *et al.* Tumor restriction by type I collagen opposes tumor-promoting effects of cancer-associated fibroblasts. *The Journal of clinical investigation* **131**, doi:10.1172/jci146987 (2021).

68 Torphy, R. J. *et al.* Stromal Content Is Correlated With Tissue Site, Contrast Retention, and Survival in Pancreatic Adenocarcinoma. *JCO precision oncology* **2018**, doi:10.1200/po.17.00121 (2018).

69 Helms, E., Onate, M. K. & Sherman, M. H. Fibroblast Heterogeneity in the Pancreatic Tumor Microenvironment. *Cancer discovery* **10**, 648-656, doi:10.1158/2159-8290.CD-19-1353 (2020).

70 Biffi, G. *et al.* IL1-Induced JAK/STAT Signaling Is Antagonized by TGFβ to Shape CAF Heterogeneity in Pancreatic Ductal Adenocarcinoma. *Cancer discovery* **9**, 282-301, doi:10.1158/2159-8290.Cd-18-0710 (2019).

71 Bernard, V. *et al.* Single-Cell Transcriptomics of Pancreatic Cancer Precursors Demonstrates Epithelial and Microenvironmental Heterogeneity as an Early Event in Neoplastic Progression. *Clinical cancer research : an official journal of the American Association for Cancer Research* **25**, 2194-2205, doi:10.1158/1078-0432.Ccr-18-1955 (2019).

72 Elyada, E. *et al.* Cross-Species Single-Cell Analysis of Pancreatic Ductal Adenocarcinoma Reveals Antigen-Presenting Cancer-Associated Fibroblasts. *Cancer discovery* **9**, 1102-1123, doi:10.1158/2159-8290.CD-19-0094 (2019).

73 Hwang, B., Lee, J. H. & Bang, D. Single-cell RNA sequencing technologies and bioinformatics pipelines. *Experimental & molecular medicine* **50**, 96, doi:10.1038/s12276-018-0071-8 (2018).

74 van den Brink, S. C. *et al.* Single-cell sequencing reveals dissociation-induced gene expression in tissue subpopulations. *Nature Methods* **14**, 935-936, doi:10.1038/nmeth.4437 (2017).

75 Biffi, G. & Tuveson, D. A. Diversity and Biology of Cancer-Associated Fibroblasts. *Physiological reviews* **101**, 147-176, doi:10.1152/physrev.00048.2019 (2021).

76 Ståhl, P. L. *et al.* Visualization and analysis of gene expression in tissue sections by spatial transcriptomics. *Science* **353**, 78, doi:10.1126/science.aaf2403 (2016).

77 Bork, P. The modular architecture of a new family of growth regulators related to connective tissue growth factor. *FEBS letters* **327**, 125-130, doi:10.1016/0014-5793(93)80155-n (1993).

78 Brigstock, D. R. *et al.* Proposal for a unified CCN nomenclature. *Molecular pathology : MP* **56**, 127-128, doi:10.1136/mp.56.2.127 (2003).

79 Jun, J.-I. & Lau, L. F. Taking aim at the extracellular matrix: CCN proteins as emerging therapeutic targets. *Nat Rev Drug Discov* **10**, 945-963, doi:10.1038/nrd3599 (2011).

80 Walsh, C. T., Stupack, D. & Brown, J. H. G protein-coupled receptors go extracellular: RhoA integrates the integrins. *Mol Interv* **8**, 165-173, doi:10.1124/mi.8.4.8 (2008).

81 Yu, S. *et al.* RU486 Metabolite Inhibits CCN1/Cyr61 Secretion by MDA-MB-231-Endothelial Adhesion. *Front Pharmacol* **10**, 1296-1296, doi:10.3389/fphar.2019.01296 (2019).

82 Lau, L. F. CCN1/CYR61: the very model of a modern matricellular protein. *Cell Mol Life Sci* **68**, 3149-3163, doi:10.1007/s00018-011-0778-3 (2011).

83 Kim, H., Son, S. & Shin, I. Role of the CCN protein family in cancer. *BMB reports* **51**, 486-492, doi:10.5483/BMBRep.2018.51.10.192 (2018).

84 Kim, K. H., Won, J. H., Cheng, N. & Lau, L. F. The matricellular protein CCN1 in tissue injury repair. *Journal of cell communication and signaling* **12**, 273-279, doi:10.1007/s12079-018-0450-x (2018).

85 Zhu, Y. *et al.* The Roles of CCN1/CYR61 in Pulmonary Diseases. *Int J Mol Sci* **21**, 7810, doi:10.3390/ijms21217810 (2020).

86 Yang, R., Chen, Y. & Chen, D. Biological functions and role of CCN1/Cyr61 in embryogenesis and tumorigenesis in the female reproductive system (Review). *Mol Med Rep* **17**, 3-10, doi:10.3892/mmr.2017.7880 (2018).

87 Hesler, R. A. *et al.* TGF-β-induced stromal CYR61 promotes resistance to gemcitabine in pancreatic ductal adenocarcinoma through downregulation of the nucleoside transporters hENT1 and hCNT3. *Carcinogenesis* **37**, 1041-1051, doi:10.1093/carcin/bgw093 (2016).

88 Holloway, S. E. *et al.* Increased expression of Cyr61 (CCN1) identified in peritoneal metastases from human pancreatic cancer. *Journal of the American College of Surgeons* **200**, 371-377, doi:10.1016/j.jamcollsurg.2004.10.005 (2005).

89 Maity, G. *et al.* Pancreatic tumor cell secreted CCN1/Cyr61 promotes endothelial cell migration and aberrant neovascularization. *Scientific reports* **4**, 4995, doi:10.1038/srep04995 (2014).

90 Haque, I. *et al.* Cyr61/CCN1 signaling is critical for epithelial-mesenchymal transition and stemness and promotes pancreatic carcinogenesis. *Mol Cancer* **10**, 8, doi:10.1186/1476-4598-10-8 (2011).

91 Maity, G. *et al.* CYR61/CCN1 Regulates dCK and CTGF and Causes Gemcitabine-resistant Phenotype in Pancreatic Ductal Adenocarcinoma. *Molecular cancer therapeutics* **18**, 788-800, doi:10.1158/1535-7163.Mct-18-0899 (2019).

92 Gao, H. *et al.* High-throughput screening using patient-derived tumor xenografts to predict clinical trial drug response. *Nature medicine* **21**, 1318-1325, doi:10.1038/nm.3954 (2015).

93 Delitto, D. *et al.* Patient-derived xenograft models for pancreatic adenocarcinoma demonstrate retention of tumor morphology through incorporation of murine stromal elements. *The American journal of pathology* **185**, 1297-1303, doi:10.1016/j.ajpath.2015.01.016 (2015).

94 Suklabaidya, S. *et al.* Experimental models of pancreatic cancer desmoplasia. *Lab Invest* **98**, 27-40, doi:10.1038/labinvest.2017.127 (2018).

95 Hidalgo, M. *et al.* Patient-derived xenograft models: an emerging platform for translational cancer research. *Cancer discovery* **4**, 998-1013, doi:10.1158/2159-8290.Cd-14-0001 (2014).

96 Hingorani, S. R. *et al.* Preinvasive and invasive ductal pancreatic cancer and its early detection in the mouse. *Cancer cell* **4**, 437-450, doi:10.1016/s1535-6108(03)00309-x (2003).

97 Hingorani, S. R. *et al.* Trp53R172H and KrasG12D cooperate to promote chromosomal instability and widely metastatic pancreatic ductal adenocarcinoma in mice. *Cancer cell* **7**, 469-483, doi:10.1016/j.ccr.2005.04.023 (2005).

98 Baker, L. A., Tiriac, H., Clevers, H. & Tuveson, D. A. Modeling pancreatic cancer with organoids. *Trends Cancer* **2**, 176-190, doi:10.1016/j.trecan.2016.03.004 (2016).

99 Bachem*, M. G. *et al.* Identification, culture, and characterization of pancreatic stellate cells in rats and humans. *Gastroenterology* **115**, 421-432, doi:10.1016/S0016-5085(98)70209-4 (1998).

100 Jesnowski, R. *et al.* Immortalization of pancreatic stellate cells as an in vitro model of pancreatic fibrosis: deactivation is induced by matrigel and N-acetylcysteine. *Lab Invest* **85**, 1276-1291, doi:10.1038/labinvest.3700329 (2005).

101 Mathison, A. *et al.* Pancreatic stellate cell models for transcriptional studies of desmoplasia-associated genes. *Pancreatology* **10**, 505-516, doi:10.1016/S1424-3903(10)80035-3 (2010).

102 Haas, S. L. *et al.* Transforming growth factor-beta induces nerve growth factor expression in pancreatic stellate cells by activation of the ALK-5 pathway. *Growth Factors* **27**, 289-299, doi:10.1080/08977190903132273 (2009).

103 Moore, P. S. *et al.* Genetic profile of 22 pancreatic carcinoma cell lines. Analysis of K-ras, p53, p16 and DPC4/Smad4. *Virchows Archiv : an international journal of pathology* **439**, 798-802, doi:10.1007/s004280100474 (2001).

104 Sipos, B. *et al.* A comprehensive characterization of pancreatic ductal carcinoma cell lines: towards the establishment of an in vitro research platform. *Virchows Archiv : an international journal of pathology* **442**, 444-452, doi:10.1007/s00428-003-0784-4 (2003).

105 Coleman, S. J. *et al.* Pancreatic cancer organotypics: High throughput, preclinical models for pharmacological agent evaluation. *World journal of gastroenterology* **20**, 8471-8481, doi:10.3748/wjg.v20.i26.8471 (2014).

106 Baker, L. A., Tiriac, H., Clevers, H. & Tuveson, D. A. Modeling pancreatic cancer with organoids. *Trends Cancer* **2**, 176-190, doi:10.1016/j.trecan.2016.03.004 (2016).

107 Loessner, D. *et al.* A 3D tumor microenvironment regulates cell proliferation, peritoneal growth and expression patterns. *Biomaterials* **190-191**, 63-75, doi:https://doi.org/10.1016/j.biomaterials.2018.10.014 (2019).

108 Tomás-Bort, E., Kieler, M., Sharma, S., Candido, J. B. & Loessner, D. 3D approaches to model the tumor microenvironment of pancreatic cancer. *Theranostics* **10**, 5074-5089, doi:10.7150/thno.42441 (2020).

109 Frappart, P.-O. & Hofmann, T. G. Pancreatic Ductal Adenocarcinoma (PDAC) Organoids: The Shining Light at the End of the Tunnel for Drug Response Prediction and Personalized Medicine. *Cancers (Basel)* **12**, 2750, doi:10.3390/cancers12102750 (2020).

110 Boj, S. F. *et al.* Organoid models of human and mouse ductal pancreatic cancer. *Cell* **160**, 324-338, doi:10.1016/j.cell.2014.12.021 (2015).

111 Tsai, S. *et al.* Development of primary human pancreatic cancer organoids, matched stromal and immune cells and 3D tumor microenvironment models. *BMC Cancer* **18**, 335, doi:10.1186/s12885-018-4238-4 (2018).

112 Fanjul, M. & Hollande, E. Morphogenesis of "duct-like" structures in three-dimensional cultures of human cancerous pancreatic duct cells (Capan-1). *In Vitro Cell Dev Biol Anim* **29A**, 574-584, doi:10.1007/BF02634151 (1993).

113 Hirschhaeuser, F. *et al.* Multicellular tumor spheroids: an underestimated tool is catching up again. *Journal of biotechnology* **148**, 3-15, doi:10.1016/j.jbiotec.2010.01.012 (2010).

114 Friedrich, J., Ebner, R. & Kunz-Schughart, L. A. Experimental anti-tumor therapy in 3-D: spheroids--old hat or new challenge? *International journal of radiation biology* **83**, 849-871, doi:10.1080/09553000701727531 (2007).

115 McLeod, E. J., Beischer, A. D., Hill, J. S. & Kaye, A. H. Multicellular tumor spheroids grown from pancreatic carcinoma cell lines: use as an orthotopic xenograft in athymic nude mice. *Pancreas* **14**, 237-248, doi:10.1097/00006676-199704000-00004 (1997).

116 Wen, Z. *et al.* A spheroid-based 3-D culture model for pancreatic cancer drug testing, using the acid phosphatase assay. *Brazilian journal of medical and biological research = Revista brasileira de pesquisas medicas e biologicas* **46**, 634-642, doi:10.1590/1414-431x20132647 (2013).

117 Yeon, S. E. *et al.* Application of concave microwells to pancreatic tumor spheroids enabling anticancer drug evaluation in a clinically relevant drug resistance model. *PLoS One* **8**, e73345, doi:10.1371/journal.pone.0073345 (2013).

118 Ware, M. J. *et al.* Generation of an in vitro 3D PDAC stroma rich spheroid model. *Biomaterials* **108**, 129-142, doi:10.1016/j.biomaterials.2016.08.041 (2016).

119 Longati, P. *et al.* 3D pancreatic carcinoma spheroids induce a matrix-rich, chemoresistant phenotype offering a better model for drug testing. *BMC Cancer* **13**, 95, doi:10.1186/1471-2407-13-95 (2013).

120 Grzesiak, J. J. & Bouvet, M. Determination of the ligand-binding specificities of the alpha2beta1 and alpha1beta1 integrins in a novel 3-dimensional in vitro model of pancreatic cancer. *Pancreas* **34**, 220-228, doi:10.1097/01.mpa.0000250129.64650.f6 (2007).

121 Gutierrez-Barrera, A. M., Menter, D. G., Abbruzzese, J. L. & Reddy, S. A. G. Establishment of three-dimensional cultures of human pancreatic duct epithelial cells. *Biochem Biophys Res Commun* **358**, 698-703, doi:10.1016/j.bbrc.2007.04.166 (2007).

122 Hosoya, H. *et al.* Engineering fibrotic tissue in pancreatic cancer: a novel three-dimensional model to investigate nanoparticle delivery. *Biochem Biophys Res Commun* **419**, 32-37, doi:10.1016/j.bbrc.2012.01.117 (2012).

123 Kunz-Schughart, L. A., Freyer, J. P., Hofstaedter, F. & Ebner, R. The Use of 3-D Cultures for High-Throughput Screening: The Multicellular Spheroid Model. *Journal of Biomolecular Screening* **9**, 273-285, doi:10.1177/1087057104265040 (2004).

124 Brancato, V. *et al.* Bioengineered tumoral microtissues recapitulate desmoplastic reaction of pancreatic cancer. *Acta biomaterialia* **49**, 152-166, doi:10.1016/j.actbio.2016.11.072 (2017).

125 Lee, J.-H. *et al.* Microfluidic co-culture of pancreatic tumor spheroids with stellate cells as a novel 3D model for investigation of stroma-mediated cell motility and drug resistance. *Journal of Experimental & Clinical Cancer Research* **37**, 4, doi:10.1186/s13046-017-0654-6 (2018).

126 Drifka, C. R., Eliceiri Kw Fau - Weber, S. M., Weber Sm Fau - Kao, W. J. & Kao, W. J. A bioengineered heterotypic stroma-cancer microenvironment model to study pancreatic ductal adenocarcinoma. *Lab Chip* **13**, 3965-3975, doi:10.1039/c3lc50487e (2013).

127 Madisen, L. *et al.* A robust and high-throughput Cre reporting and characterization system for the whole mouse brain. *Nature neuroscience* **13**, 133-140, doi:10.1038/nn.2467 (2010).

128 Strell, C. *et al.* Stroma-regulated HMGA2 is an independent prognostic marker in PDAC and AAC. *British journal of cancer* **117**, 65-77, doi:10.1038/bjc.2017.140 (2017).

129 Norberg, K. J. *et al.* A novel pancreatic tumour and stellate cell 3D co-culture spheroid model. *BMC Cancer* **20**, 475, doi:10.1186/s12885-020-06867-5 (2020).

130 Bankhead, P. *et al.* QuPath: Open source software for digital pathology image analysis. **7**, 16878, doi:10.1038/s41598-017-17204-5 (2017).

131 Conway, T. *et al.* Xenome--a tool for classifying reads from xenograft samples. *Bioinformatics* **28**, i172-i178, doi:10.1093/bioinformatics/bts236 (2012).

132 Dobin, A. *et al.* STAR: ultrafast universal RNA-seq aligner. *Bioinformatics* **29**, 15-21, doi:10.1093/bioinformatics/bts635 (2012).

133 Liao, Y., Smyth, G. K. & Shi, W. featureCounts: an efficient general purpose program for assigning sequence reads to genomic features. *Bioinformatics* **30**, 923-930, doi:10.1093/bioinformatics/btt656 (2014).

134 McCarthy, D. J., Chen, Y. & Smyth, G. K. Differential expression analysis of multifactor RNA-Seq experiments with respect to biological variation. *Nucleic Acids Research* **40**, 4288-4297, doi:10.1093/nar/gks042 %J Nucleic Acids Research (2012).

135 Liberzon, A. *et al.* The Molecular Signatures Database (MSigDB) hallmark gene set collection. *Cell systems* **1**, 417-425, doi:10.1016/j.cels.2015.12.004 (2015).

136 Kanehisa, M. & Goto, S. KEGG: kyoto encyclopedia of genes and genomes. *Nucleic Acids Res* **28**, 27-30, doi:10.1093/nar/28.1.27 (2000).

137 Tiriac, H. *et al.* Organoid Profiling Identifies Common Responders to Chemotherapy in Pancreatic Cancer. *Cancer discovery* **8**, 1112-1129, doi:10.1158/2159-8290.Cd-18-0349 (2018).

138 Kolde, R. *pheatmap: Pretty Heatmaps. R package version 1.0.12.*, <https://CRAN.R-project.org/package=pheatmap> (2019).

139 Davis, S. & Meltzer, P. S. GEOquery: a bridge between the Gene Expression Omnibus (GEO) and BioConductor. *Bioinformatics* **23**, 1846-1847, doi:10.1093/bioinformatics/btm254 (2007).

140 Wickham, H. ggplot2: Elegant Graphics for Data Analysis. *Springer-Verlag New York* (2016).

141 Bartholin, L., Wessner, L. L., Chirgwin, J. M. & Guise, T. A. The human Cyr61 gene is a transcriptional target of transforming growth factor beta in cancer cells. *Cancer letters* **246**, 230-236, doi:https://doi.org/10.1016/j.canlet.2006.02.019 (2007).

142 Sakamoto, S. *et al.* Increased Expression of CYR61, an Extracellular Matrix Signaling Protein, in Human Benign Prostatic Hyperplasia and Its Regulation by Lysophosphatidic Acid. *Endocrinology* **145**, 2929-2940, doi:10.1210/en.2003-1350 %J Endocrinology (2004).

143 Miyabayashi, K. *et al.* Intraductal Transplantation Models of Human Pancreatic Ductal Adenocarcinoma Reveal Progressive Transition of Molecular Subtypes. *Cancer discovery* **10**, 1566-1589, doi:10.1158/2159-8290.CD-20-0133 (2020).

144 Hayashi, A. *et al.* A unifying paradigm for transcriptional heterogeneity and squamous features in pancreatic ductal adenocarcinoma. *Nature Cancer* **1**, 59-74, doi:10.1038/s43018-019-0010-1 (2020).

145 Somerville, T. D. D. *et al.* TP63-Mediated Enhancer Reprogramming Drives the Squamous Subtype of Pancreatic Ductal Adenocarcinoma. *Cell Rep* **25**, 1741-1755.e1747, doi:10.1016/j.celrep.2018.10.051 (2018).

146 Guo, J. A. *et al.* Refining the Molecular Framework for Pancreatic Cancer with Single-cell and Spatial Technologies. *Clinical cancer research : an official journal of the American Association for Cancer Research* **27**, 3825-3833, doi:10.1158/1078-0432.CCR-20-4712 (2021).

147 Aung, K. L. *et al.* Genomics-Driven Precision Medicine for Advanced Pancreatic Cancer: Early Results from the COMPASS Trial. *Clinical cancer research : an official journal of the American Association for Cancer Research* **24**, 1344-1354, doi:10.1158/1078-0432.CCR-17-2994 (2018).

148 Porter, R. L. *et al.* Epithelial to mesenchymal plasticity and differential response to therapies in pancreatic ductal adenocarcinoma. *Proceedings of the National Academy of Sciences of the United States of America* **116**, 26835-26845, doi:10.1073/pnas.1914915116 (2019).

149 Richards, K. E. *et al.* Cancer-associated fibroblast exosomes regulate survival and proliferation of pancreatic cancer cells. *Oncogene* **36**, 1770-1778, doi:10.1038/onc.2016.353 (2017).

150 Toste, P. A. *et al.* Chemotherapy-Induced Inflammatory Gene Signature and Protumorigenic Phenotype in Pancreatic CAFs via Stress-Associated MAPK. *Molecular cancer research : MCR* **14**, 437-447, doi:10.1158/1541-7786.Mcr-15-0348 (2016).

151 Provenzano, P. P. *et al.* Enzymatic targeting of the stroma ablates physical barriers to treatment of pancreatic ductal adenocarcinoma. *Cancer cell* **21**, 418-429, doi:10.1016/j.ccr.2012.01.007 (2012).

152 Zhang, D. *et al.* Tumor-Stroma IL1β-IRAK4 Feedforward Circuitry Drives Tumor Fibrosis, Chemoresistance, and Poor Prognosis in Pancreatic Cancer. *Cancer research* **78**, 1700-1712, doi:10.1158/0008-5472.CAN-17-1366 (2018).

153 Dalin, S. *et al.* Deoxycytidine Release from Pancreatic Stellate Cells Promotes Gemcitabine Resistance. *Cancer research* **79**, 5723-5733, doi:10.1158/0008-5472.CAN-19-0960 (2019).

154 Olive, K. P. *et al.* Inhibition of Hedgehog signaling enhances delivery of chemotherapy in a mouse model of pancreatic cancer. *Science* **324**, 1457-1461, doi:10.1126/science.1171362 (2009).

155 Banasik, M. B. & McCray, P. B. Integrase-defective lentiviral vectors: progress and applications. *Gene Therapy* **17**, 150-157, doi:10.1038/gt.2009.135 (2010).

156 Ui-Tei, K. Optimal choice of functional and off-target effect-reduced siRNAs for RNAi therapeutics. *Front Genet* **4**, 107-107, doi:10.3389/fgene.2013.00107 (2013).

157 Waise, S. *et al.* An optimised tissue disaggregation and data processing pipeline for characterising fibroblast phenotypes using single-cell RNA sequencing. *Scientific reports* **9**, 9580, doi:10.1038/s41598-019-45842-4 (2019).

158 Carter, M. & Shieh, J. in *Guide to Research Techniques in Neuroscience (Second Edition)* (eds Matt Carter & Jennifer Shieh) 295-310 (Academic Press, 2015).

159 Lenggenhager, D. *et al.* Commonly Used Pancreatic Stellate Cell Cultures Differ Phenotypically and in Their Interactions with Pancreatic Cancer Cells. *Cells* **8**, doi:10.3390/cells8010023 (2019).

160 Sun, J. *et al.* Comprehensive RNAi-based screening of human and mouse TLR pathways identifies species-specific preferences in signaling protein use. *Sci Signal* **9**, ra3-ra3, doi:10.1126/scisignal.aab2191 (2016).

161 Zheng-Bradley, X., Rung, J., Parkinson, H. & Brazma, A. Large scale comparison of global gene expression patterns in human and mouse. *Genome Biol* **11**, R124-R124, doi:10.1186/gb-2010-11-12-r124 (2010).

162 O'Kane, G. M. *et al.* GATA6 Expression Distinguishes Classical and Basal-like Subtypes in Advanced Pancreatic Cancer. *Clinical cancer research : an official journal of the American Association for Cancer Research* **26**, 4901-4910, doi:10.1158/1078-0432.Ccr-19-3724 (2020).

163 Nicolle, R. *et al.* A transcriptomic signature to predict adjuvant gemcitabine sensitivity in pancreatic adenocarcinoma. *Annals of oncology : official journal of the European Society for Medical Oncology* **32**, 250-260, doi:10.1016/j.annonc.2020.10.601 (2021).

164 Mitsunaga, S. *et al.* Serum levels of IL-6 and IL-1β can predict the efficacy of gemcitabine in patients with advanced pancreatic cancer. *British journal of cancer* **108**, 2063-2069, doi:10.1038/bjc.2013.174 (2013).

165 Hwang, W. L. *et al.* Single-nucleus and spatial transcriptomics of archival pancreatic cancer reveals multi-compartment reprogramming after neoadjuvant treatment. *bioRxiv*, 2020.2008.2025.267336, doi:10.1101/2020.08.25.267336 (2020).

166 Dominguez, C. X. *et al.* Single-Cell RNA Sequencing Reveals Stromal Evolution into LRRC15(+) Myofibroblasts as a Determinant of Patient Response to Cancer Immunotherapy. *Cancer discovery* **10**, 232-253, doi:10.1158/2159-8290.Cd-19-0644 (2020).